Graphical Abstract

A two-level approach for multi-objective flexible job shop scheduling and energy procurement

Sascha Christian Burmeister, Daniela Guericke, Guido Schryen

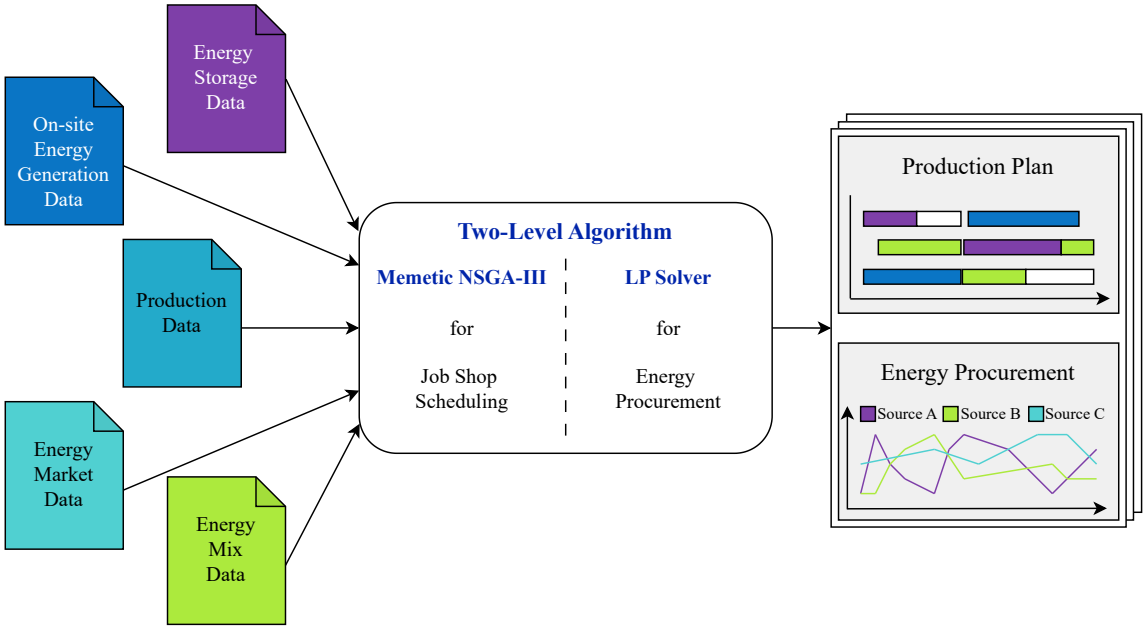

Highlights

A two-level approach for multi-objective flexible job shop scheduling and energy procurement

Sascha Christian Burmeister, Daniela Guericke, Guido Schryen

- Integrating scheduling with energy procurement improves production sustainability
- Production planning can respond to changes of dynamic energy prices and emissions
- Seasonal differences affect potential savings in energy cost and emissions
- Decision-makers can vary makespan, costs, and emissions based on their preferences
- Pareto fronts enable balancing production efficiency and sustainability

A two-level approach for multi-objective flexible job shop scheduling and energy procurement

Sascha Christian Burmeister[a,*], Daniela Guericke[b], Guido Schryen[a]

[a] *Paderborn University, Warburger Str. 100, Paderborn, 33098, NRW, Germany*
[b] *University of Twente, Drienerlolaan 5, Enschede, 7522NB, The Netherlands*

Abstract

Dynamic energy tariffs in combination with energy storage systems (ESS) and renewable energy sources (RES) offer manufacturers new opportunities to optimize their energy consumption. Flexible production planning empowers decision-makers not only to minimize makespan, but also to reduce energy costs and emissions. However, flexible production planning is a major challenge due to the fact that scheduling decisions affect energy demand, whose costs and emissions depend on energy procurement decisions. In Operations Research, the Green Flexible Job Shop Scheduling Problem (FJSP) addresses production planning decisions incorporating resource, environmental, and economic objectives. The Energy Procurement Problem (EPP) aims to efficiently acquire energy resources. In the literature, existing approaches for energy-aware scheduling neglect to procure energy from sources such as an uncertain dynamic energy market, RES, and ESS. We aim to close this research gap and propose a two-level approach based on a memetic Non-dominated Sorting Genetic Algorithm (NSGA-III) and linear programming with the goal of minimizing the makespan, energy costs, and emissions of a schedule, incorporating dynamic energy prices and emissions, RES, and ESS. We evaluate the approach in computational experiments using FJSP benchmark instances from the literature as part of a rolling horizon approach with real energy market data. We investigate the impact of RES and ESS by presenting estimated Pareto fronts, showing potential savings in energy cost and carbon emissions.

Keywords: Energy-aware Scheduling, Metaheuristic, Manufacturing, Multiple Objectives, Energy procurement

*Corresponding author
Email addresses: sascha.burmeister@upb.de (Sascha Christian Burmeister), d.guericke@utwente.nl (Daniela Guericke), guido.schryen@upb.de (Guido Schryen)

Preprint accepted for publication in Cleaner Energy Systems *January 27, 2025*

1. Introduction

The use of renewable energy plays a key role in addressing the increasingly pressing issue of climate change. In 2021, renewable sources account for roughly 34% of the total energy generation in Europe, and this sector is expected to grow further, promoted by ambitious climate goals, technological progress, and policy incentives (Elbersen et al., 2012; Hassan et al., 2024). Since renewable energy generation, such as wind and solar power, is uncertain and volatile, a significant challenge involves balancing energy supply and demand to increase the use of renewable energy (Warren, 2014). One method to improve the utilization of renewable energy is a flexible alignment of energy consumption (Panda et al., 2023). This study investigates demand response of manufacturers by addressing flexible production planning integrated with energy procurement decisions considering the following aspects.

First, manufacturers can employ flexible production planning, adjusting their production to external factors such as current energy prices and emissions and to their own energy generation, with the goal of minimizing makespan, energy costs, and emissions. Additionally, energy-intensive processes beyond production, such as combined heat and power generation or cooling buildings in an industrial context, can also be integrated into production planning (Mitra et al., 2013; Mancò et al., 2024; Barco-Burgos et al., 2022). While traditional energy tariffs feature fixed purchase prices, Time-of-Use (TOU) tariffs offer a solution by setting the price based on the time of day (such as on-peak and off-peak). Real-Time Pricing (RTP) tariffs are dynamic energy tariffs involving price adjustments at least on an hourly basis, e.g., in alignment with the day-ahead market price developments. By scheduling energy-intensive processes during periods characterized by low energy costs, and vice versa, manufacturers can benefit from cost savings when improving production flexibility in combination with implementing RTP tariffs (Körner et al., 2019). Apart from lowering energy cost, emissions reduction can also be an objective of flexible production planning: As an exogenous influence, dynamic price signals are one approach to incentivize the shift of energy demand to periods of high generation of renewable energy (Huang et al., 2019; Jordehi, 2019). Endogenously motivated, manufacturers can direct their focus towards the emissions of the current energy market, scheduling energy-intensive processes based on the energy mix of the market to align with corporate sustainability goals (Maia et al., 2022).

Second, manufacturers can improve energy procurement to meet their demand, including their own energy sources and storage systems in addition to grid power. Incorporating behind-the-meter renewable energy sources (RES) such as solar pan-

els or wind turbines can amplify the effects of cost and emissions savings, while targeted control of Energy Storage Systems (ESS) further enhances the flexibility of energy consumption (Obi et al., 2020; Yasmin et al., 2024). Studies show that large electricity consumers can significantly reduce their energy costs through strategic energy procurement decisions (Conejo et al., 2005; Beraldi et al., 2017). Zhang et al. (2016) and Leo et al. (2021) further demonstrate the benefit of integrating electricity procurement with production scheduling.

However, manufacturers face several challenges when adopting flexible production planning. Production planning decisions must be synchronized with decisions for energy procurement from RES, ESS, and the grid, especially since different decision-makers (e.g. production planner and energy procurement manager) are usually involved here. In addition, uncertainties must be considered in both the energy market-dependent scheduling and the use of RES and ESS. Varying external factors, such as weather conditions and day-ahead market for the coming day, together with associated renewable energy generation from wind and solar sources, can affect energy cost and production emissions. Additionally, when rescheduling production plans due to changing external factors, past scheduling decisions are irreversible and cannot be altered.

To align production scheduling and energy procurement with the energy market, we address (1) the Flexible Job Shop Problem (FJSP) and (2) the Energy Procurement Problem (EPP): (1) Job-shop scheduling problems assign a given set of jobs with different processing times to a set of machines to minimize the makespan (Zhang et al., 2019). A job can consist of multiple operations that must be processed sequentially. In a flow shop problem (FSP), machines are given as n-tuples and each job is divided into n operations, such that each machine is specialized for exactly one operation. In an FJSP, a machine can be specialized for multiple operations such that an operation can be processed by any machine in a given set. (2) The EPP focuses on efficient acquisition of energy resources and aims to minimize energy procurement expenses. It incorporates various energy sources, including self-generated energy from RES and ESS, bilateral contracts such as power purchase agreements, and spot markets, to determine the optimal energy mix required to meet energy demands at the lowest possible cost (Beraldi et al., 2017).

As we show in Section 2, several approaches to energy-aware scheduling have been studied in the literature. However, previous studies focus on specific aspects, resulting in limited coverage. To the best of our knowledge, there is no multi-objective approach that simultaneously addresses the minimization of makespan, energy cost, and emissions, while considering the uncertainties of a dynamic energy market and utilizing on-site energy from RES and ESS.

The objective of this work is to develop and evaluate a multi-objective scheduling approach that simultaneously minimizes makespan, energy cost, and emissions while accounting for the uncertainties of a dynamic energy market and utilizing on-site renewable energy and energy storage systems. We aim to provide decision-makers with insights into the potential energy cost and emissions savings achievable through enhanced production flexibility. To assess our approach through computational experiments, we study its performance under various conditions. Our analysis examines the effects of seasonal differences, the influence of decision-makers on how much they want to respond to dynamic energy prices and emissions, and the suitability of our approach and its results for practical use. The primary research questions guiding our analysis are:

I How do different seasonal conditions affect potential savings in energy cost and emissions?

II To what extent can decision-makers influence the makespan, energy cost, and emissions of schedules?

III How feasible are energy costs and emission-based schedules for practice?

Our contribution entails three main components: (1) formulating linear optimization models to solve the FJSP and EPP for the multi-objective minimization of makespan, dynamic energy cost and emissions; (2) developing a novel Memetic algorithm inspired by NSGA-III; and (3) conducting comprehensive computational experiments to analyze reductions in energy cost and emissions.

The remainder of this paper is structured as follows. Section 2 presents related work to our contribution and highlights the research gap. Section 3 outlines the mathematical formulations for the FJSP and the EPP. Section 4 describes the solution approach to solve the FJSP and EPP. Section 5 presents the details and experimental setup used for evaluation and discusses the results of our computational experiments. Sections 6.1 through 6.3 present and discuss the results of our experiments related to the research questions I through III. Section 7 summarizes our work and gives an outlook for future research.

2. Related Work

In this section, we introduce the existing literature on energy-aware scheduling. We categorize recent studies based on their objectives, energy aspects considered, the type of problem addressed, the developed model, and the solution approach. The

Table 1: Related work

Author	Objective					Energy Aspects				Problem		Model	Approach[1]
	Makespan	Emissions	Energy Cost	Energy Consumption	Peak Consumption	Energy Rate	ESS	RES	Uncertain Energy Data	Stages	Type	Type	Approach
Gong et al. (2018)	●			●						M	FJSP	MINLP	H
Gong et al. (2021)	●			●						M	FJSP	MIP	H
Yin et al. (2017)	●			●						M	FJSP	MIP	H
Wu and Sun (2018)	●			●						M	FJSP	MINLP	H
Lu et al. (2021)	●			●						M	FJSP	MIP	H
Dai et al. (2019)	●			●						M	FJSP	MIP	H
Li et al. (2020)	●	●								M	FJSP	MIP	H
Wu et al. (2018)	●	●					●	●		M	FSP	MINLP	H
Fang et al. (2011)	●	●			●					M	FSP	MIP	E
Jiang et al. (2019)	●		●							S		MIP	H
Cui et al. (2019)			●		●	TOU	●	●	❍	M	FSP	MINLP	H
Ding et al. (2015)			●			TOU				S		MIP	H
Che et al. (2017)			●			TOU				S		MIP	E
Moon and Park (2014)			●			TOU	●	●		M	FJSP	MIP	E
Biel et al. (2018)			●			TOU		●	❍	M	FSP	SMIP	E
Zhang et al. (2017)			●			TOU	●	●		S		MIP	E
Duarte et al. (2020)			●			TOU	●	●	❍	S		SMIP	E
Wang et al. (2020a)	●		●			TOU				M	FJSP	MIP	H
Masmoudi et al. (2019)	●		●			TOU				S		MIP	E
Chen et al. (2022)	●		●			TOU	●	●	❍	M	HFSP	MIP	H
Karimi and Kwon (2021)	●		●			TOU	●	●		S		MIP	E
Wang et al. (2020b)	●		●			TOU	●	●	❍	M	FSP	SMIP	E
Jabeur et al. (2024)			●			TOU	●	●		M	FJSP	MIP	H
Dong and Ye (2022)	●	●	●			TOU	●	●	❍	M	FSP	MIP	H
Zhang et al. (2014)		●	●			TOU				M	FSP	MIP	E
Zhang et al. (2015)			●			RTP				M	FSP	MIP	E
Lee et al. (2017)			●			RTP				S		MINLP	H
Abikarram et al. (2019)			●			RTP				S		MIP	E
Shrouf et al. (2014)			●			RTP				S		MIP	H
Gong et al. (2015)			●			RTP				S		MIP	E
Gong et al. (2016)			●			RTP				S		MIP	H
Zhai et al. (2017)			●			RTP		●		M	FSP	MIP	E
Fazli Khalaf and Wang (2018)			●			RTP	●	●	●	M	FSP	SMIP	E
Golpîra et al. (2018)			●		●	RTP	●	●	❍	M	JSP	SMIP	E
Schulz et al. (2019)	●		●		●	RTP				M	FSP	MIP	H
Burmeister et al. (2023)	●		●			RTP				M	FJSP	MIP	H
Burmeister (2024)	●	●	●			RTP				M	FJSP	MIP	H
This study	●	●	●			RTP	●	●	●	M	FJSP	MIP	H

●: The aspect is considered ❍: The aspect is partly considered
[1]E: Exact method, H: Heuristic approach [2]S: Single stage, M: Multiple stages

literature reviewed in Table 1 focuses on scheduling approaches that consider aspects related to energy and is conceptually sorted according to the objective.

First, we discuss the objective of the related work in Table 1. There are multiple studies that minimize both makespan and overall energy consumption by adjusting production speed, scheduling idle times, or turning off machines (Gong et al., 2018, 2021; Yin et al., 2017; Wu and Sun, 2018; Lu et al., 2021; Dai et al., 2019). Li et al. (2020), Wu et al. (2018), and Fang et al. (2011) incorporate sustainable concepts in their studies by focusing on emissions rather than energy consumption. Fang et al. (2011) supplements the minimization of makespan and emissions with the minimization of peak consumption as a third objective to map and reduce associated costs. The remaining studies in Table 1 consider the minimization of energy costs as an objective. Many studies examine the minimization of energy cost as the sole optimization goal in designing energy-efficient schedules for decision-makers (Ding et al., 2015; Che et al., 2017; Moon and Park, 2014; Biel et al., 2018; Zhang et al., 2017; Duarte et al., 2020; Zhang et al., 2015; Lee et al., 2017; Abikarram et al., 2019; Shrouf et al., 2014; Gong et al., 2015, 2016; Zhai et al., 2017; Fazli Khalaf and Wang, 2018). The objective of minimizing energy costs is also integrated into multi-objective optimization alongside other goals. Some studies aim to further reduce energy costs by including considerations for expenses related to peak energy consumption (Cui et al., 2019; Golpîra et al., 2018). Another common combination of objectives is the minimization of both makespan and energy costs (Jiang et al., 2019; Wang et al., 2020a; Masmoudi et al., 2019; Chen et al., 2022; Karimi and Kwon, 2021; Wang et al., 2020a; Burmeister et al., 2023). Minimizing the makespan and energy cost yield solutions that not only entail low energy costs but also ensure short production times. Instead of concentrating on makespan, Zhang et al. (2014) minimize both energy costs and emissions, ensuring schedules that are cost-effective and sustainable. Dong and Ye (2022) and Burmeister (2024) adopt a three-criteria approach with the aim of designing schedules that are efficient in terms of makespan, energy cost, and emissions, thus combining the aforementioned objectives in one model.

Second, we delve into the energy aspects examined in the research, focusing on (1) energy tariff, (2) utilization of RES and ESS, and (3) handling of uncertain energy data. (1) While Jiang et al. (2019) minimize energy costs assuming constant energy prices, many publications focus on TOU tariffs (Ding et al., 2015; Che et al., 2017; Biel et al., 2018; Moon and Park, 2014; Zhang et al., 2017; Duarte et al., 2020; Zhang et al., 2014; Karimi and Kwon, 2021; Wang et al., 2020a,b; Masmoudi et al., 2019; Chen et al., 2022). They divide a day into different time periods (e.g. off-peak, mid-peak, and on-peak) with different energy costs. In contrast to studies under the assumption of constant prices or TOU rates, the remaining studies aiming at mini-

mizing energy cost opt for RTP rates (Zhang et al., 2015; Shrouf et al., 2014; Gong et al., 2015, 2016; Zhai et al., 2017; Fazli Khalaf and Wang, 2018; Golpîra et al., 2018; Schulz et al., 2019; Burmeister et al., 2023; Burmeister, 2024). Compared with TOU tariffs, RTP tariffs stand out for their finer temporal resolution, dividing a day into, e.g. hourly segments instead of a few broad periods. RTP prices change dynamically and do not repeat daily as TOU prices. The increased dynamic provides additional opportunities to reduce energy costs by redistributing production. However, complexity increases with the length of the planning horizon considered because of the large number of time steps. (2) With regard to RES sources, Zhai et al. (2017) and Biel et al. (2018) both assume wind energy generation and formulate their models to allow the utilization of the energy generated for cost-effective production. Every other study reviewed that considers RES also introduces ESS (Wu et al., 2018; Cui et al., 2019; Moon and Park, 2014; Zhang et al., 2017; Duarte et al., 2020; Chen et al., 2022; Karimi and Kwon, 2021; Wang et al., 2020b; Dong and Ye, 2022; Fazli Khalaf and Wang, 2018; Golpîra et al., 2018). By introducing ESS, renewable and cost-efficiently generated energy can be stored and utilized for later consumption. (3) With regard to the consideration of uncertainties in the energy data, there are different approaches in the considered studies. In Table 1, we mark the aspect of uncertain energy data as partially met in the studies of Cui et al. (2019), Biel et al. (2018), Duarte et al. (2020), Chen et al. (2022), Wang et al. (2020b), Dong and Ye (2022), and Golpîra et al. (2018). These studies consider uncertainties with respect to RES, e.g. changing forecasts of available wind or solar power. However, they neglect the dynamics of an energy market, which are considered in the work of Fazli Khalaf and Wang (2018). Here, the authors consider various scenarios involving RTP energy prices and RES generation, thus addressing the discrepancies between predicted and actual renewable energy supply.

Third, we discuss the problem types and the classes of models developed. Among the studies reviewed in Table 1, the authors predominantly consider multistage FSPs and FJSPs. Studies including time-dependent energy costs more frequently choose the setting of a single machine problem. This may be due to the fact that a formulation with time-indexed variables is required to represent time-dependent energy costs, which are less efficient compared to sequence-position or precedence variables. Gong et al. (2018), Wu and Sun (2018), Wu et al. (2018), Cui et al. (2019), and Lee et al. (2017) formulate nonlinear models to represent generated emissions, the interaction of TOU tariffs and peak demand costs, or energy measures in the objective function. All other studies considered choose linear formulations. Biel et al. (2018), Duarte et al. (2020), Wang et al. (2020b), Fazli Khalaf and Wang (2018), and Golpîra et al. (2018) develop stochastic models to deal with uncertainties in future

energy production. Cui et al. (2019) adopts a rolling horizon approach in which they update uncertain weather data daily and adjust schedules to changing conditions.

Fourth, we discuss the solution approach of the reviewed literature. Exact solution methods are used, e.g., in Che et al. (2017), Zhang et al. (2017), or Karimi and Kwon (2021), which solve a single-stage scheduling problem. Heuristic and metaheuristic approaches are predominantly found in the considered studies, which could be related to the fact that the FJSP belongs to the class of NP-hard problems (Garey et al., 1976). Jiang et al. (2019) use variable neighborhood search, while Schulz et al. (2019) use local search. Gong et al. (2018) and Wu and Sun (2018) use an evolutionary algorithm. Memetic metaheuristics are used in Wu et al. (2018), Wang et al. (2020a) and Burmeister et al. (2023).

The reviewed literature place different emphases in the area of energy-aware scheduling. We identify the research gap that there is no work yet that guides manufacturers to develop schedules that consider makespan, energy cost, and low emissions while while accounting for the uncertain real-time energy market, along with behind-the-meter RES and ESS. Considering these aspects is important, as the three objectives might conflict. Furthermore, focusing solely on the grid is insufficient, as incorporating local resources can substantially impact both energy cost and sustainability. We intend to extend the research with a novel approach that guides manufacturers in creating schedules while simultaneously recommending short-term energy procurement decisions (i.e. day-ahead market, utilization of self-production) depending on current RES generation, ESS levels, and the RTP energy market.

3. Optimization models

In this section, we present the multi-objective optimization problem. Section 3.1 introduces the formulation of the energy-aware FJSP, accounting for scheduling aspects such as job start times and machine allocations. Section 3.2 presents the formulation of the EPP, addressing aspects of energy procurement to meet the energy demand resulting from the FJSP.

3.1. Energy-aware FJSP formulation

In this section, we present the multi-objective energy-aware FJSP to minimize makespan, energy cost, and emissions. Table 2 shows the notation of the model. The model is based on the work of Burmeister (2024) and the general FJSP formulation of Özgüven et al. (2010).

Set J comprises the jobs to be processed, while the set $O_i = \{(i,1), ..., (i,\nu_i)\}$ subdivides each job i into ν_i operations that must be processed in sequence. Set

$O = \bigcup_{i \in J} O_i$ unites all operations of all jobs. Set $M = \{1, ..., \xi\}$ contains all available machines. Parameter τ_{ijk} specifies the duration for processing an operation (i, j) on machine k. Set $T = \{1, ..., \theta\}$ contains the time steps. The parameters η_{ijkt} and ζ_{ijkt} indicate the energy costs and emissions, respectively, caused by processing operation (i, j) on machine k when processing is started at time step t.

Table 2: Notation for the energy-aware FJSP model

Notation	Description
Sets	
J	Jobs, $i, i' \in J$
O_i	Operations of job i, $(i, j) \in O_i$, $O_i = \{(i, 1), ..., (i, \nu_i)\}$
O	Operations, $O = \bigcup_{i \in J} O_i$,
M	Machines, $k \in M$
T	Time steps, $t \in T$
Parameters	
τ_{ijk}	Processing time of operation (i, j) on machine k
ρ_{ijkt}	Energy demand for processing operation (i, j) on machine k when starting at time t
η_t	Energy cost at time t
ζ_t	Energy emissions at time t
$u_{c^{max}}$	Upper bound for the maximum makespan
L	A large number
Variables	
c^{max}	Maximum makespan
p^{sum}	Sum of all energy cost
e^{sum}	Sum of all emissions
d_t	Energy demand at time t
s_{ijk}	Start time of operation (i, j) on machine k
c_{ijk}	End time of operation (i, j) on machine k
x_{ijk}	Binary indicator, 1 iff operation (i, j) is allocated on machine k
$y_{iji'j'k}$	Binary indicator, 1 iff job j, operation j is predecessor of job i', operation j' on machine k
α_{ijkt}	Binary indicator, 1 iff operation (i, j) starts on machine k at time t
β_{ijkt}	Binary indicator, 1 iff operation (i, j) runs on machine at time t

Equation (1) defines the three-criteria objective function for minimizing makespan c^{max}, energy cost p^{sum}, and emissions e^{sum}. Equation (2) defines makespan as the time at which the last operation (i, j) was completed for all machines k. Equation (3) limits the maximum allowed makespan to parameter $u_{c^{max}}$. If the multi-criteria objective function is weighted and no focus is placed on the makespan, this constraint helps prevent an unbounded model by avoiding the indefinite postponement of operation start times. Equation (4) ensures the assignment of each operation (i, j) to exactly one machine k. Equation (5) ensures that if an operation (i, j) is assigned to a

machine k, its start time s_{ijk} and end time c_{ijk} are established correctly. Equation (6) ensures that the operation- and machine-dependent processing time elapses between the start and end time. Simultaneously, Equation (7) prevents an operation starting before the previous operation ended. Equivalent to Equations (6) and (7), Equations (8) and (9) prevent a machine k from concurrently processing distinct operations. Equation (10) ensures that exactly one variable α_{ijkt} indicates the start of operation (i, j) on machine k for a time t, if and only if variable x_{ijk} indicates the operation's assignment to this machine. Equations (11) and (12) ensure that the indicator α_{ijkt} is linked to the start time s_{ijk}. Equation (13) ensures that the binary variable β_{ijkt} indicates whether operation (i, j) is running on machine k at time t, based on the values of α_{ijkt} within the time span from $t - \tau_{ijk}$ to t. Equation (14) aggregates the total energy demand in all operations and machines at each time step t.

$$
\begin{aligned}
&\min\ (c^{max}, p^{sum}, e^{sum}) && && (1)\\
&\text{s.t. } c^{max} \geq c_{ijk} && \forall i,j,k && (2)\\
&\quad c^{max} \leq u_{c^{max}} && && (3)\\
&\quad \sum_{k} x_{ijk} = 1 && \forall i,j && (4)\\
&\quad s_{ijk} + c_{ijk} \leq x_{ijk} L && \forall i,j,k && (5)\\
&\quad c_{ijk} \geq s_{ijk} + \tau_{ijk} - (1 - x_{ijk}) L && \forall i,j,k && (6)\\
&\quad \sum_{k} s_{ijk} \geq \sum_{k} c_{i,j-1,k} && \forall i,j && (7)\\
&\quad s_{ijk} \geq c_{i'j'k} - y_{iji'j'k} L && \forall i,j,i',j',k && (8)\\
&\quad s_{i'j'k} \geq c_{ijk} - (1 - y_{iji'j'k}) L && \forall i,j,i',j',k && (9)\\
&\quad x_{ijk} = \sum_{t} \alpha_{ijkt} && \forall i,j,k && (10)\\
&\quad s_{ijk} - t \geq -(1 - \alpha_{ijkt}) L && \forall i,j,k,t && (11)\\
&\quad s_{ijk} - t \leq (1 - \alpha_{ijkt}) L && \forall i,j,k,t && (12)\\
&\quad \sum_{t-\tau_{ijk}}^{t} \alpha_{ijkt} \leq \beta_{ijkt} && \forall i,j,k,t \geq \tau_{ijk} && (13)\\
&\quad d_t \geq \sum_{ijk} \rho_{ijk} \beta_{ijkt} && \forall t && (14)
\end{aligned}
$$

$$c^{max}, p^{sum}, e^{sum}, s_{ijk}, c_{ijk} \in \mathbb{R}_+,$$
$$x_{ijk}, y_{iji'j'k}, \alpha_{ijkt}, \beta_{ijkt} \in \{0,1\} \qquad \forall i,j,i',j',k,t \tag{15}$$

The model is an MILP due to its incorporation of both binary and continuous variables within linear constraints. The size of the model depends upon the cardinality of the sets of operations O, machines M, and time steps T. The set of jobs J does not directly impact the size, as the constraints associated with a job i are related to its operations $(i,j) \in O$. The number of variables is $|O|^2 \cdot |M| + 2 \cdot |O| \cdot |M| \cdot |T| + 3 \cdot |O| \cdot |M| + |T| + 3$. The number of constraints is $2 \cdot |O|^2 \cdot |M| + 3 \cdot |O| \cdot |M| \cdot |T| + 4 \cdot |O| \cdot |M| + 2 \cdot |O| + |T| + 1$.

3.2. EPP formulation

In this section, we present the multi-objective EPP for minimizing energy costs and emissions. Table 3 shows the notation of the model. The sets R and S contain the available RES and ESS technologies, respectively. The set T contains the time steps.

Table 3: Notation for the EPP model

Notation	Description
Sets	
R	RES, $r \in R$
S	ESS, $s \in S$
T	Time steps, $t \in T$
Parameters	
d_t	Energy demand at time t
p_t^g	Energy cost for grid energy at time t
e_t^g	Emissions for grid energy at time t
p_{rt}^{res}	Energy cost for RES r at time t
e_{rt}^{res}	Emissions for RES r energy at time t
p_{st}^{ess}	Energy cost for ESS s at time t
e_{st}^{ess}	Emissions for ESS s energy at time t
u_{rt}^h	Energy generation of source r at time t
l_s^λ, u_s^λ	Lower and upper bound for the level of ESS s
u_s^γ, u_s^δ	Upper bounds for charging and discharging ESS s
w_s	Relative energy losses for discharging ESS s
Variables	
p^{sum}	Sum of all energy cost
e^{sum}	Sum of all emissions
g_t	Grid consumption at time t
h_{rt}	Consumption from source r at time t
λ_{st}	Level of ESS s at time t
γ_{st}	Energy charged into ESS s at time t
δ_{st}	Energy discharged from ESS s at time t

Equation (16) defines the two-criteria objective function to minimize the cost for purchasing energy from the grid p_t (Equation (17)) and emissions e_t (Equation (18)) for each time step t. Equation (19) ensures an energy balance by accounting for the energy input from the grid g_t, RES generation h_{rt}, and discharging the ESS δ_{st} in relation to the energy demand d_t and charging for the ESS for all RES r and ESS s. The energy demand d_t is calculated based on the production schedule resulting from the model Equation (1)-Equation (15). The energy discharged from the ESS takes into account losses based on a relative factor w_s. Equation (20) states that the model starts with an empty ESS at time $t = 0$. For further time steps $t > 0$, Equation (21) calculates the respective ESS state-of-charge level λ_{st}, which results from the level of the previous time step $\lambda_{s,t-1}$ plus charging γ_{st} and minus discharging δ_{st}. Equation (22) ensures that the ESS level remains within the specified bounds l_s^λ and u_s^λ. Equations (23) and (24) limit the amount of energy that can be charged (γ_{st}) to or discharged (δ_{st}) from the ESS per time step to the upper bounds u_s^γ and u_s^δ, respectively. Equation (25) limits the energy sourced from RES to the quantity generated for each time step t.

$$\min \ (p^{sum}, e^{sum}) \tag{16}$$

$$\text{s.t. } p^{sum} \geq \sum_t \left(p_t^g g_t + \sum_r p_{rt}^{res} h_{rt} + \sum_s p_{st}^{ess} \delta_{st} \right) \tag{17}$$

$$e^{sum} \geq \sum_t \left(e_t^g g_t + \sum_r e_{rt}^{res} h_{rt} + \sum_s e_{st}^{ess} \delta_{st} \right) \tag{18}$$

$$g_t + \sum_r h_{rt} + w_s \sum_s \delta_{st} = d_t + \sum_s \gamma_{st} \qquad \forall t \tag{19}$$

$$\lambda_{st} = 0 \qquad \forall s, t = 0 \tag{20}$$

$$\lambda_{s,t-1} + \gamma_{st} - \delta_{st} = \lambda_{st} \qquad \forall s, t > 0 \tag{21}$$

$$l_s^\lambda \leq \lambda_{st} \leq u_s^\lambda \qquad \forall s, t \tag{22}$$

$$\gamma_{st} \leq u_s^\gamma \qquad \forall s, t \tag{23}$$

$$\delta_{st} \leq u_s^\delta \qquad \forall s, t \tag{24}$$

$$h_{rt} \leq u_{rt}^h \qquad \forall r, t \tag{25}$$

$$g_t, \lambda_{st}, \gamma_{st}, \delta_{st}, h_{rt} \in \mathbb{R}_+ \qquad \forall r, s, t \tag{26}$$

The model contains only continuous variables in linear constraints and is classified as an LP. The size of the model depends on the cardinality of the sets of RES R,

ESS S, and the time steps T. The number of variables is given by $3 \cdot |S| \cdot |T| + \cdot |R| \cdot |T| + |T| + 2$. The number of constraints is $4 \cdot |S| \cdot |T| + \cdot |R| \cdot |T| \cdot |T| + 2$.

4. Solution Approach

This section describes a novel decoupling strategy to address energy scheduling and procurement challenges. Our approach reduces the complexity of the two-level model by separating energy scheduling and procurement decisions. The FJSP is addressed using a Memetic NSGA-III, while the EPP is solved exactly in a subsequent phase with a solver. To manage uncertainties, the method is embedded within a Rolling Horizon framework, facilitating dynamic and iterative solution updates, thereby improving its practical applicability and overall effectiveness.

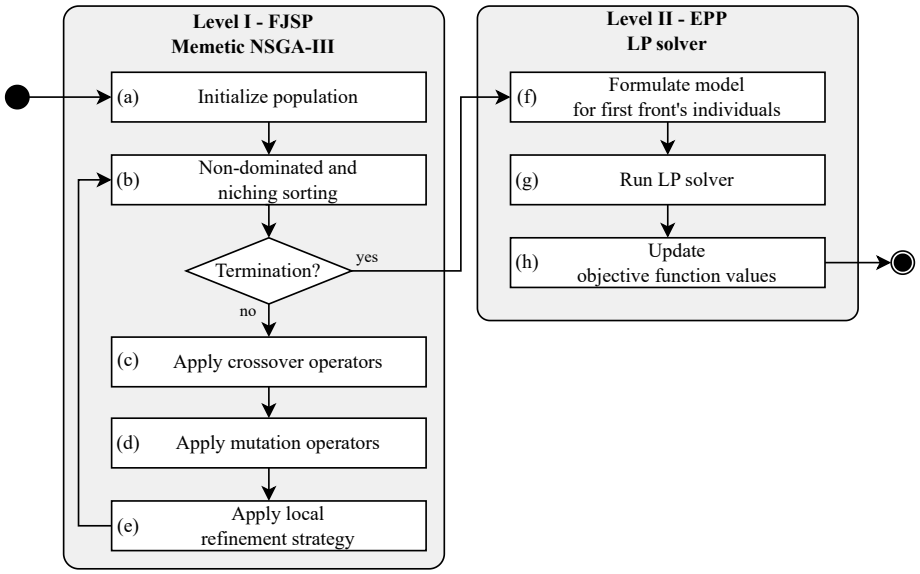

Figure 1: Flow chart diagram of the two-level algorithm

Figure 1 shows the process of our two-level approach. In the first phase the algorithm (a) initializes a population and (b) sorts it using the non-dominated niching sorting method proposed by Deb and Jain (2013). Until termination criteria are met, the algorithm proceeds with (c) crossover and (d) mutation operators. Subsequently, (e) a local refinement strategy is applied to improve energy cost and emissions while maintaining the makespan, effectively transforming NSGA-III into a memetic algorithm.

In the second phase, we determine the short-term energy procurement needed to meet the energy demand generated by the schedule developed in the first phase.

Because the mathematical formulation of EPP is linear, we opt for an exact solution and (f) formulate a Linear Programming (LP) model for every individual of the estimated Pareto front. The models are (g) run on a solver, accounting for the energy demand of the first phase's solutions, the current RES generation, ESS levels, and the day-ahead market. The last step involves (h) retrieving the solutions from the solver and computing the final energy cost and emissions based on the optimal procurement decisions. These results are then presented to the decision-maker, who selects the preferred schedule from among the available choices.

Section 4.1 presents the Memetic NSGA-III, which focuses on optimizing schedules and determining when to utilize energy from the grid and RES, and when to charge or discharge available ESS. Section 4.2 justifies the use of a rolling horizon framework to address uncertainty and presents how we embed the two-level approach in such a framework.

4.1. Memetic NSGA-III

In this subsection, we describe the Memetic NSGA-III. We use the NSGA-III as a basis for a memetic evolutionary algorithm adapted to the problem, because it has shown to be successful on problems with three to five objectives (Deb and Jain, 2013). In the literature, there are also alternatives to NSGA-III, such as θ-DEA (Yuan et al., 2015), which aims to improve the convergence ability of NSGA-III in high-dimensional objective spaces, or NTGA2 (Myszkowski and Laszczyk, 2021), which focuses on diversity promotion by separate treatment of objective dimensions in combinatorial many-objective problems (i.e., four or more objectives, Ishibuchi et al. (2008)). Given that the problem considered has only three objectives, we choose to adhere to NSGA-III.

In addition, Memetic NSGA-III calculates a solution front, allowing decision makers to choose a solution from a set of solutions according to their individual preferences. This eliminates the need for scalarization, where the multi-objective problem is simplified into a single-objective problem, e.g., using methods such as the weighted sum or weighted Tchebycheff methods, which yield only one solution (Li et al., 2019).

Section 4.1.1 introduces the representation of the problem as a genotype and phenotype. Section 4.1.2 introduces greedy refinement as a memetic component.

4.1.1. Representation

As an evolutionary algorithm, the Memetic NSGA-III conceptualizes solutions as individuals within a population that progress across numerous generations. We adopt a decoder-based approach from Burmeister (2024) to depict solutions as individuals. A genotype encodes an individual as a chromosome, while a phenotype decodes a chromosome to an individual.

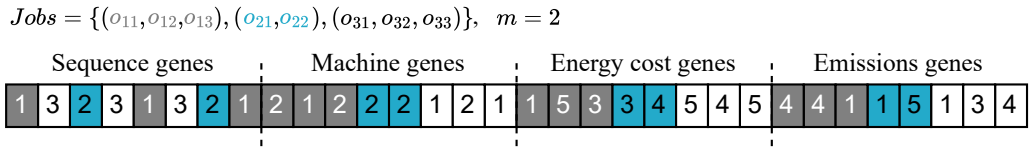

Figure 2: Example genotype for solution encoding (Burmeister, 2024)

Figure 2 shows an example genotype that consists of four chromosomes, each the length of the number of operations. Sequence genes determine the sequencing of job operations, dictating their order of execution. Machine genes, on the other hand, govern the allocation of operations to specific machines. Meanwhile, energy cost and emission genes define the acceptable thresholds for costs or emissions during operation execution.

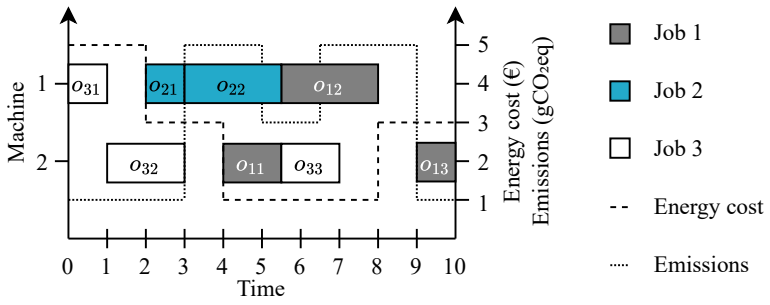

Figure 3: Representation of the example genotype as a phenotype (Burmeister, 2024)

In Figure 3, the example genotype is depicted as a phenotype. Time intervals are marked on the x-axis, while machines are delineated on the left y-axis. The energy cost values, presented as a dashed line, and emissions values, represented as a dotted line, are indicated on the right y-axis. Energy costs are expressed in €/MWh, while emissions are quantified in grams of carbon dioxide equivalent (gCO_2eq) per kWh. The first sequence gene indicates that an operation of job 1 is assigned first, while the associated machine gene specifies assignment to machine 2. Consequently, the operation $(1, 1)$ is assigned to machine 2 and scheduled at the earliest available time that meets both the prescribed maximum allowable energy cost and emissions criteria specified by the respective gene strings.

4.1.2. Greedy refinement

A local refinement strategy extends NSGA-III to a memetic algorithm. We adopt a greedy refinement strategy from the work of Burmeister (2024) and outline the al-

gorithm in Algorithm 1. The algorithm adjusts the energy cost and emission genes of randomly selected individuals to minimize energy costs and emissions while preserving the same sequence and machine genes as well as the same makespan. To achieve this, the operations L (including their machine assignment) of a parent are sorted by their energy consumption in descending order and duplicated into two sets, L_c, for the children $c \in \{1, 2\}$. The algorithm then iterates over each operation $(i, j) \in L_c$ and determines the earliest and latest possible start times l_{cij} and u_{cij} based on the preceding and succeeding operations. The functions `GetTimeOfMinCostBetween` and `GetTimeOfMinEmissionBetween` are employed to ascertain a time s_{cij} between l_{cij} and u_{cij} at which the operation can be scheduled to minimize either energy cost (for $c = 1$) or emissions (for $c = 2$). When all operations are scheduled, the algorithm is terminated, and both children are added to the population. The local refinement strategy follows a greedy nature and prioritizes scheduling energy-intensive operations first, aiming to achieve savings in energy cost and emissions.

Algorithm 1 Pseudocode of the greedy refinement

Require: Operations L (sorted by energy consumption in descending order)
  for all Children $c \in \{1, 2\}$ **do**
    $L_c \leftarrow$ copy of L
    for $\iota \leftarrow 0$ to $|L_c| - 1$ **do**
      $l_{cij} \leftarrow$ earliest possible start time for $(i, j) \in L_c$
      $u_{cij} \leftarrow$ latest possible start time for $(i, j) \in L_c$
      if c is 1 **then**
        $s_{cij} \leftarrow$ GetTimeOfMinCostBetween(l_{cij}, u_{cij})
      else
        $s_{cij} \leftarrow$ GetTimeOfMinEmissionBetween(l_{cij}, u_{cij})
      end if
      Schedule $L_c[\iota]$ at s_{cij}
    end for
  end for

4.2. Rolling Horizon

In this section, we discuss uncertainty aspects and present the rolling horizon approach. In contrast to alternative methods, such as probabilistic approaches that require reliable probability distributions or robust techniques that depend on deterministic or set-based uncertainty modeling, the rolling horizon approach dynamically incorporates updated information from subsequent periods. This is achieved by periodically decomposing and solving the problem, enabling refined decision-making in response to evolving data (Bertsimas et al., 2011; Wang et al., 2019; Glomb et al.,

2022). Glomb et al. (2022) conceptualize the rolling horizon problem as a finite sequence of coupled optimization problems $\{P_1, ...P_T\}$, where each problem belongs to a time $t \in [T] := \{0, ..., T\}$. They partition the variables of a problem P_t into three sets: Start state variables Ξ_t, interior variables X_t, and end state variables Θ_t. The start-state variables of one time period must correspond to the end-state variables of the previous period to establish a connection between adjacent periods. The objective function consists only of interior variables that are used solely within a specific time period. The primary advantage of a rolling horizon approach lies in its ability to manage uncertainties by continuously updating forecasts and integrating newly available information at each decision stage, enabling more informed and adaptive decision-making (Glomb et al., 2022). Although it may lead to suboptimal solutions due to its reliance on limited planning horizons and sequential decision-making, this approach can substantially reduce computational time compared to traditional methods and give good solutions in reasonable computation time (Marquant et al., 2015; Glomb et al., 2022).

In the context of the FJSP and the EPP, uncertainty stems from exchange-dependent energy prices and weather- and demand-driven emissions associated with the energy mix. For the day-ahead market, the prices and associated energy sources for the initial 24 hours are fixed, while data beyond remain unknown. Given the cyclical announcement of the following day's values, we adopt a rolling horizon approach, working with known day-ahead energy costs and emissions, as well as uncertain forecasts for the future. This enables us to adjust decisions on a daily basis and finalize decisions for the upcoming day using newly available information on energy costs and emissions, as well as updated forecasts.

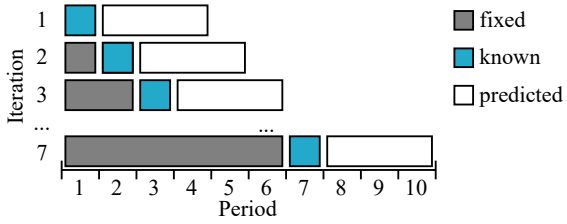

Figure 4: Illustration of a rolling horizon

Figure 4 illustrates a rolling horizon process with 10 periods and 7 iterations. In the first step, decisions are made for the first time period using both known data for that period and anticipated data for subsequent periods. The decisions are then fixed as they relate to past events. Iteratively, anticipated values for the next period are updated, forecasts for future periods are refined, and missing data is supplemented.

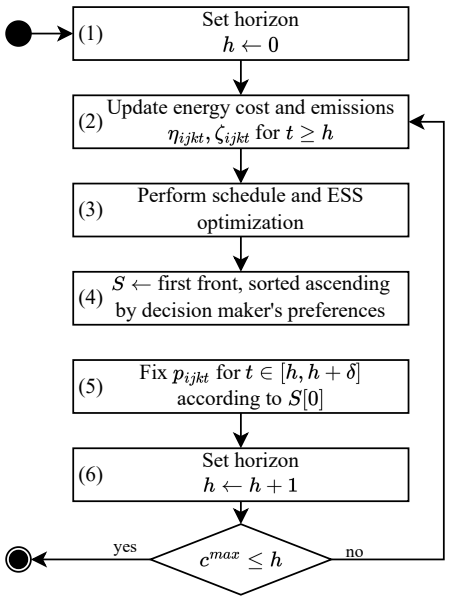

Figure 5: Flow chart diagram of the rolling horizon

Figure 5 illustrates the adaptation of rolling horizon to our two-level algorithm. The variable h denotes the current horizon considered, while δ represents the duration of this horizon. As depicted in the activity diagram, the process begins at the horizon $h = 0$ in step (1). In step (2), the energy cost and emissions parameters (η_{ijkt} and ζ_{ijkt}) are set to the presently known or predicted values. In step (3), the algorithm performs the schedule and EPP optimization with the given energy cost and emission values as described in Section 4.1. In step (4), the decision-maker select their preferred solution S from the computed Pareto front. In step (5), all variables α_{ijkt} within the horizon, spanning from h to $h + \delta$, are fixed before incrementing the horizon h in step (6). The procedure continues with the initialization of the subsequent iteration in step (2) until all operations are assigned such that $c^{max} \leq h$.

5. Computational Experiments

In this section, we outline the design of our computational experiments. Section 5.1 presents the evaluation instances used. To address the research questions I to III introduced in Section 1, we consider cases, that we present in Section 5.2. Section 5.3 introduces the experiment setting.

5.1. Instances

For the evaluation of our algorithm, we use the set of benchmarks from Brandimarte (1993). The set is shown in Table 4 and contains 15 instances for the FJSP with jobs and their respective operations, as well as machines, making it suitable for emulating a production schedule. These benchmark instances allow a consistent and comparable evaluation of our results, ensuring that the algorithm's performance can be assessed under standardized conditions.

Table 4: Benchmark instances by Brandimarte (1993)

Instance	Jobs	Machines	Operations per job	Operations in total	Time steps per operation	Time step scaling (in min)
mk01	10	6	5-7	55	1-7	60
mk02	10	6	5-7	58	1-7	60
mk03	15	8	10	150	1-20	30
mk04	15	8	3-10	90	1-10	60
mk05	15	4	5-10	106	5-10	30
mk06	10	10	15	150	1-10	60
mk07	20	5	5	100	1-20	60
mk08	20	10	5-10	225	5-20	15
mk09	20	10	10-15	240	5-20	15
mk10	20	15	10-15	240	5-20	30
mk11	30	5	5-8	179	10-30	15
mk12	30	10	5-10	193	10-30	15
mk13	30	10	5-10	231	10-30	15
mk14	30	15	8-12	277	10-30	15
mk15	30	15	8-12	284	10-30	30

To place the cases in a realistic context of dynamic energy costs and emissions, we assign each operation $i \in J$ an increasing energy consumption of $160 + \frac{i}{|J|} 600$ kW, e.g., the first operation of the first job from instance mk01 has a consumption of 160 kW, while the last operation of the last job consumes 760 kW. To derive processing times from the generic time steps, we choose an associated duration of 15 to 60 minutes for each instance in such a way that solutions may yield a makespan of less than 10 days. We choose this scaling with the intention of allowing the algorithm to compute up to 10 horizons, in order to be able to observe the evolution of solutions over time.

For each instance, we assume that an ESS with a capacity of 1200 kWh is available for use. The ESS can be charged and discharged at rates of 25 and 30 kW, respectively, with an assumed storage loss of 5%. We also assume that behind-the-meter solar panels and wind turbines are available with a maximum generation of

6000 kWp for solar and 3500 kWp for wind. The values are based on real ESS and RES.

5.2. Cases

To evaluate instances (cf. Section 5.1) within a realistic context and to address the research questions I to III posed in Section 1, we design cases for solving the instances. As a case, we define changing seasonal conditions, encompassing developments in energy prices and emissions in the energy market, as well as different solar and wind conditions and the resulting amount of self-generated electricity. Additionally, a case specifies the decision-making rule that guides how a decision-maker selects a schedule at the end of a horizon as part of the rolling horizon process. The decision-making rule is referred to as the decision-maker's trajectory in the following discussion. Table 5 presents an overview of all case settings.

Table 5: Case settings

Characteristic	Value	Description
Season		
January	Jan 04 to 14, 2021	German wholesale energy
March	Mar 22 to Apr 01, 2021	price and emissions data
May	May 03 to 13, 2021	used
Trajectory		
MS	min makespan	The assumed preference of
EC	min energy cost	the decision-maker to select
EM	min emissions	a solution for the next
TO	best trade-off	decision horizon

To assume cases with realistic characteristics of the energy market, we select three 10-day intervals from January, March, and May 2021, using authentic data sourced from the Federal Network Agency Germany (2024). The January period characterizes a cold and dark season, while May represents its warm and sunny counterpart. The March period falls in between, forming a moderate season. To represent realistic characteristics of on-site solar and wind energy generation data, we scale the energy market values for solar and wind generation to the assumed kWp for behind-the-meter RES. Figure 6a illustrates energy prices for the March season, Figure 6b shows the emissions, and Figure 6c shows the RES generation. The x-axes reflect the respective date and time, with the y-axes displaying costs in €/MWh, emissions in grams of carbon dioxide equivalent (gCO_2eq) per kWh, and kW generated, respectively. The solid lines represent actual past values, while the

dashed lines depict the predicted values assumed at the beginning of each day for the decision horizons. This implies that for the initial decision horizon, the algorithm has access to data up to March 22 and uses forecasts starting March 23. In the subsequent horizon, data for March 22 and 23 are available, and the forecast from March 24 onwards is utilized, and this pattern continues. Appendix A presents the January and May period and further details about calculation of forecasts.

Our algorithm generates an estimated Pareto front of non-dominated schedules and associated procurement plans, allowing the decision-maker to select a suitable solution based on individual preferences a posteriori. The selected solution serves as the starting point for the subsequent decision horizon in the rolling horizon framework. Given that schedules span multiple days in each experiment, it is necessary to define distinct trajectories to simulate various decision-makers at the end of a planning horizon. To account for diverse decision-making styles, we consider four different trajectories, including three extreme cases: a first decision-maker prioritizing minimum makespan (MS), a second one prioritizing minimum energy cost (EC), and a third one prioritizing minimum emissions (EM). Additionally, we define a fourth decision-maker that prefers a trade-off (TO) trajectory, where the objective function values for the three objectives are normalized, and the solution closest to the utopian point $(0, 0, 0)$ is selected. Regarding energy procurement, for the MS, EC, and TO trajectories, energy cost minimization is assumed for the EPP; for the EM trajectory, emission minimization is assumed.

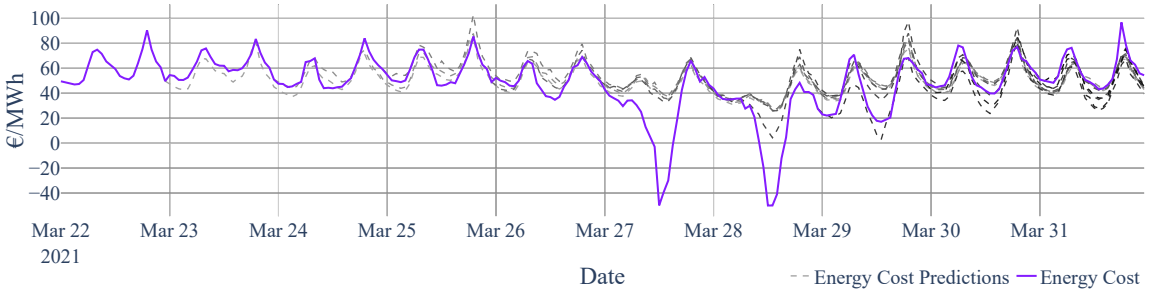

(a) Energy cost

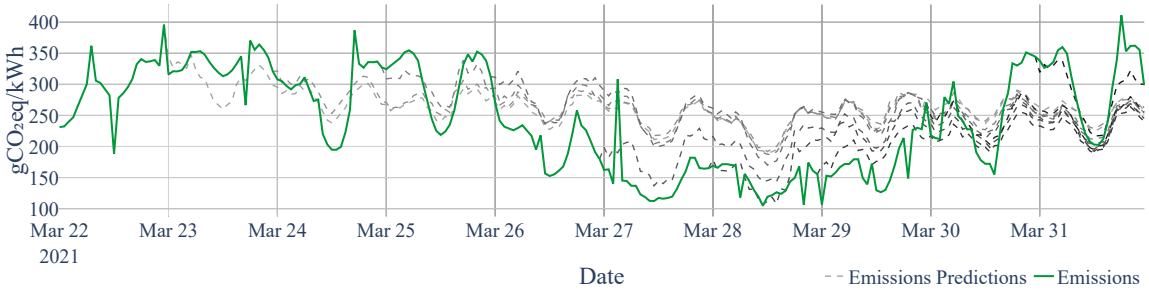

(b) Emissions

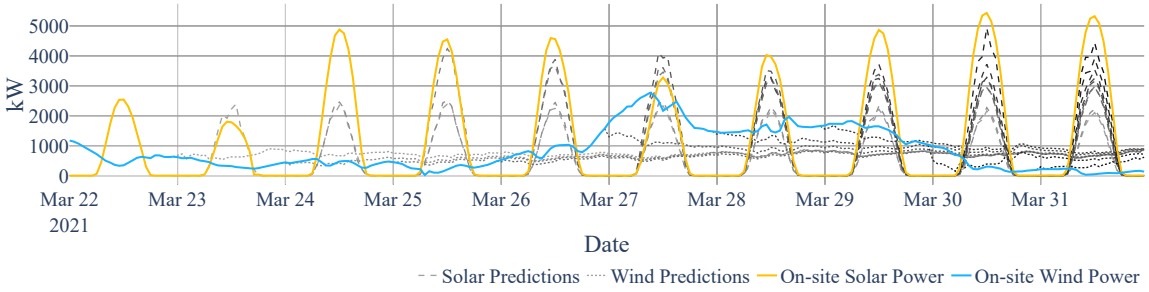

(c) Solar and wind generation

Figure 6: Energy data and predictions for March season

5.3. Experimental Setting

For computational experiments, Memetic NSGA-III is implemented in C# 12.0 within the .NET 8 software framework. For exact solving of the EPP, we use the Gurobi 11.0.0 solver with a relative MIP optimality gap of 0.0001. For the Memetic NSGA-III, we adopt the parameterization of Burmeister et al. (2023), with detailed explanations provided in the referenced study. The problem is solved on a Red Hat Enterprise Linux 8.6 (Oopta) operating system with an Intel Xeon Gold 6148 CPU, 20x2.4 GHz, 80 GByte main memory and a run-time limitation of 30 minutes per run.

6. Results

In this section, we investigate the results for each of the research questions I-III as stated in Section 1. Section 6.1 examines the effects of seasonal differences. Section 6.2 explores the effects of different trajectories. Section 6.3 assesses the practicality of the schedules resulting from our approach. Given that the Memetic NSGA-III incorporates random values, we perform ten repetitions to solve each instance. Unless otherwise specified, average values for each of the ten repetitions are presented in Sections 6.1 to 6.3.

6.1. Effects of seasonal differences

In this section, we refer to the research question I and evaluate the effects of different seasonal differences on the values of the objective function. The results presented in this section are computed under the assumption that the decision-maker follows a trade-off trajectory. To determine the impact of different seasons, Figures 7a to 7c show scatter plots for the three objective function values makespan, energy cost, and emissions. The x-axis represents the 15 instances, while the y-axis indicates the corresponding objective function values. Each marker represents the objective function value that can be achieved based on the day-ahead market conditions and the associated generation of renewable energy from wind and solar sources for the months of January, March and May 2021. See Appendix B for detailed results for all instances.

Figure 7a shows the average makespan values in different instances from 10 runs categorized by season. The lowest makespan values are achieved in the May season for 14 out of 15 instances, with the remaining instance (mk02) showing the lowest makespan in March. For instances with fewer than 20 jobs (mk01-mk06), the differences in the makespan range from 6.44% (2.8 time steps, mk02) to 21.5% (15.3 time steps, mk01) with a median of 13.13% (19.8 time steps). In contrast, in instances with at least 20 jobs (mk07-mk15), the makespan differs by 7.21% (33.9 time steps, mk15) to 22.93% (89.2 time steps, mk10) with a median of 13.11% (86.5 time steps). The lowest standard deviation across the 10 different runs is observed for instance mk02 during the May season, measuring 3.27 time steps. In contrast, the highest deviation occurs for instance mk09 in the January season, reaching 52.08 time steps.

Figure 7b shows the average energy costs in different instances categorized by season. For all instances, the algorithm can find the schedules with the lowest energy costs for the May season. For instances with fewer than 20 jobs, 67.32% (€1073.77, mk02) to 92.04% (€4763.91, mk06) of the energy cost are saved in the May season compared to the season with the highest energy cost, with a median of 86.89% (€4058.31). For instances with at least 20 jobs, the savings in energy cost amount

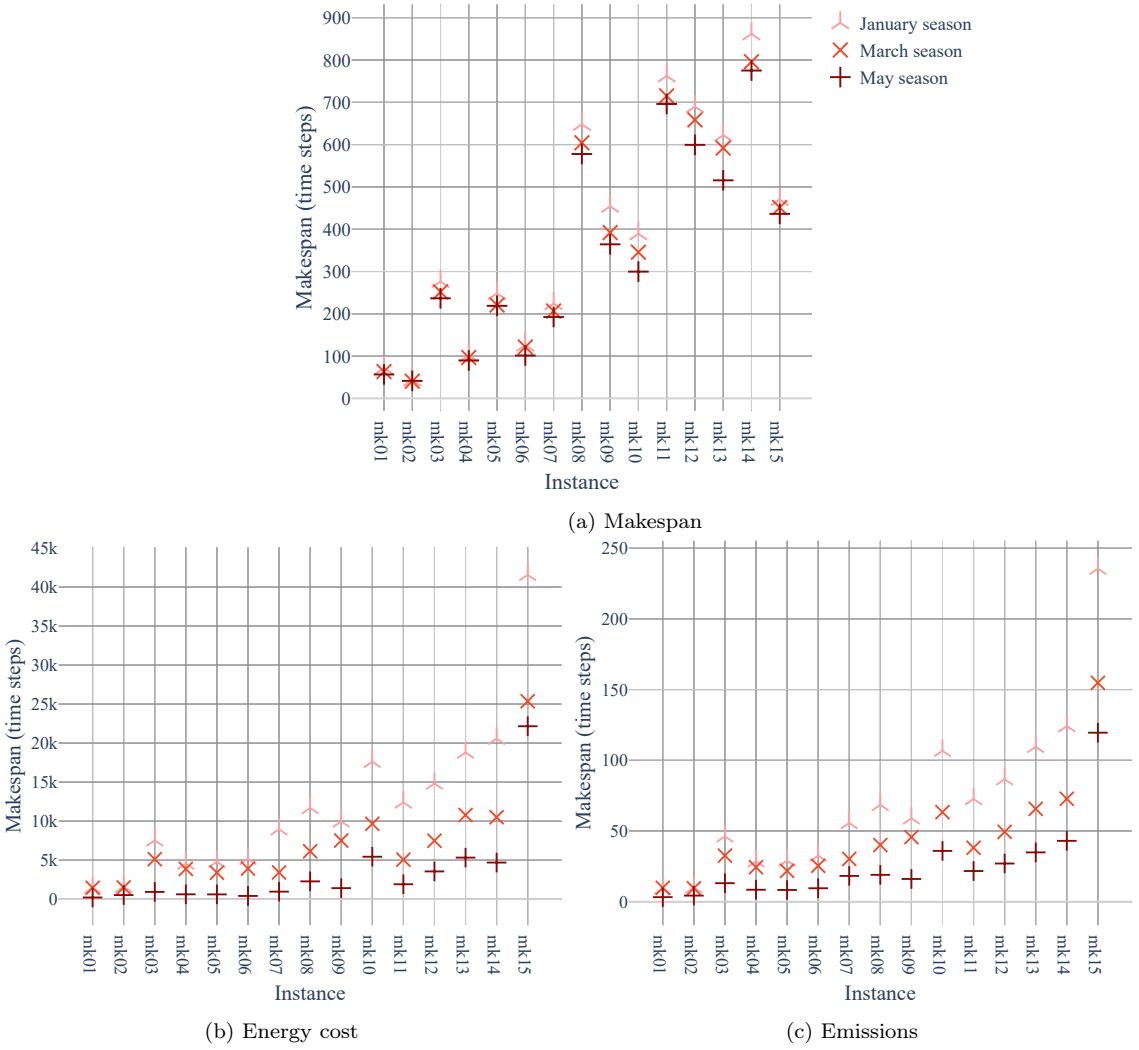

(a) Makespan

(b) Energy cost

(c) Emissions

Figure 7: Objective function values subject to seasonal conditions

to between 46.68% (€19397.89, mk15) and 89.28% (€7992.56, mk07) with a median of 77.21% (€11258.51). The lowest standard deviation across the 10 different runs is observed for instance mk02 during the March season, measuring €94.53. In contrast, the highest deviation occurs for instance mk15 in the May season, reaching €1622.03. Figure 7c shows the average emissions across different instances categorized by season. The results are similar to those for energy costs, with savings of up to 72.80% (42.92 t, mk09) in percentage terms and up to 115.99 t (49.25%, mk15) CO_2eq in absolute terms. The lowest standard deviation across the 10 different runs is observed

for instance mk01 during the May season, measuring 0.32 t CO_2eq. In contrast, the highest deviation occurs for instance mk10 in the January season, reaching 7.02 t CO_2eq.

With regard to the research question I – how seasonal conditions affect scheduling and energy procurement – the results show that seasonal differences significantly impact the final energy cost and emissions of schedules. This can be attributed to the significantly higher availability of solar and wind energy during the spring and summer seasons compared to January. Although from an intuitive perspective, energy generation should not directly impact the makespan, it is reduced as a result of the decision-maker's trajectory selection for the experiments. When following a trade-off trajectory in the spring and summer seasons, lower energy prices and fewer emissions combined with a higher amount of energy generated by RES lead to lower energy costs and emissions. As a result, the Pareto fronts identified in our experiments demonstrate lower maximum energy costs and emissions, and consequently, their knee point also reflects a decreased makespan. The findings in this section quantify these differences and highlight their impact on overall energy costs, supporting the results of other studies that emphasize that considering renewable energy availability in production scheduling has a significant impact on energy cost and emissions savings (Fazli Khalaf and Wang, 2018; Dong and Ye, 2022).

6.2. Effects of decision trajectories

In this section, we refer to the research question II and analyze how different trajectories influence the characteristics of schedules. The results presented in this subsection are computed given the day-ahead market conditions of the March season. Since we have introduced the trajectories to mimic decision-makers' choices for schedules for the end of each horizon, we investigate the progression of objective function values over multiple horizons of the rolling-horizon approach. To provide a detailed view, we focus on two selected instances, which represent a medium and large size instance with 20 and 30 jobs, respectively. Appendix C provides a complete presentation of all diagrams and detailed results for all instances.

Figures 8 and 9 show the progression of objective function values retrospectively over several horizons of the rolling-horizon approach for instances mk10 and mk14. Since we chose a horizon length of one day, horizon 0 reflects the anticipated objective function value for scheduling all jobs and all days at the end of the first day, while the final objective function values are shown at each curve's endpoint. If a line ends before the last horizon, all operations have been processed and the procedure has terminated. The color of a line represents the decision-makers' trajectory: black lines represent an MS trajectory, purple lines depict an EC trajectory, green lines depict

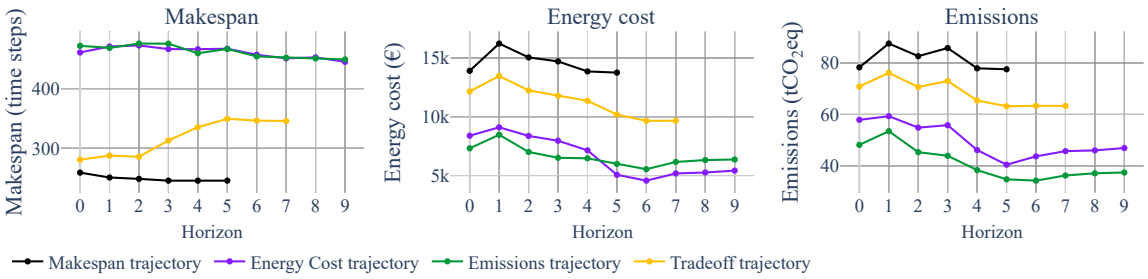

Figure 8: Objective values of instance mk10 for different trajectories over multiple horizons

an EM trajectory, and yellow lines depict an TO trajectory.

Figure 8 shows the objective function values for instance mk10 for 10 runs. The average makespan values range between 245.5 time steps when following the MS trajectory and 345.7, 445.1, and 449.2 time steps when following the TO, EC, and EM trajectory, respectively. The standard deviations for makespan measure 5.06, 16.99, 14.81, and 16.00 time steps, respectively. As the Memetic NSGA-III algorithm is provided with additional opportunities to refine the schedule with each horizon, the average makespan of the runs with MS trajectory decreases from an initial 259 time steps after horizon 0 to a final 245.5 time steps after horizon 5. The findings on energy costs demonstrate that the EC trajectory yields the lowest costs, averaging €5417.41, which are 43.91% less than those of the TO trajectories (€9658.75). The standard deviations for energy cost measure €931.14 for EC trajectory and €1462.28 for TO trajectory. In terms of emissions, the EM trajectory results in the lowest emissions (37.42 tCO_2eq), a 20.24% deviation from the EC trajectory emissions (46.92 t) and a 40.88% deviation from the TO trajectory emissions (74.97 t). The standard deviations for emissions are 3.31 t for EM trajectory and 6.35 t $_2$eq for TO trajectory. Opting out of the MS trajectory could potentially lead to savings of up to 60.60% in energy costs when following the EC trajectory and up to 51.73% in emissions when following the EM trajectory. Both cases would be accompanied by an increase in makespan of 66.67%.

Figure 9 shows the results for instance mk14. The MS trajectory achieves a makespan of 694.00 time steps, while the TO, EC and EM trajectories require 796.0, 921.7, and 930.9 time steps, respectively. The standard deviations for makespan measure 0, 20.13, 10.68, and 15.25 time steps, respectively. The EC trajectory incurs energy costs of €6514.26, while the TO, EM, and MS trajectories result in costs of €10502.53, €8291.06, and €10075.37, respectively. The standard deviations for energy costs are €672.59, €678.49, €704.16, and €318.52, respectively. In terms of emissions, the EM trajectory emits an average of 52.10 tCO_2eq, while the TO, EC,

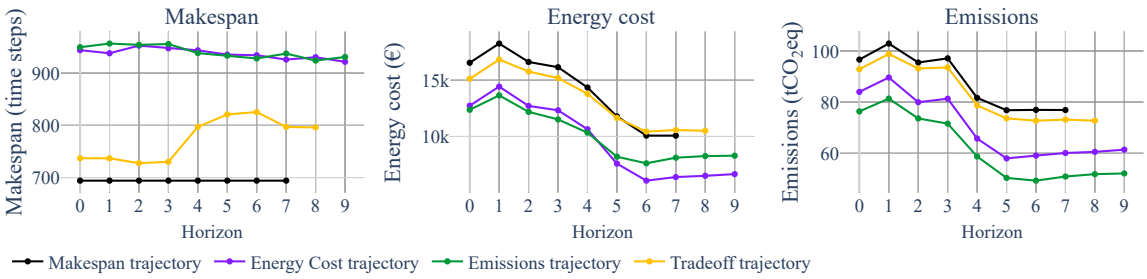

Figure 9: Objective values of instance mk14 for different trajectories over multiple horizons

and MS trajectories emit 75.19 t, 61.40 t, and 76.91 t, respectively. The standard deviations for emissions are 2.21 t, 2.13 t, 1.70 t, and 1.39 t CO_2eq, respectively. Opting out of the MS trajectory could potentially lead to savings of up to 33.94% in energy costs and up to 32.26% in emissions.

With regard to the research question II – in what ways decision-makers can influence the outcomes through different trajectories – the results show that trajectories applied during the rolling horizon approach have a significant impact on the final schedule. This can be explained by the fact that schedules are fixed by previous decision horizons during their iterative calculation in the rolling horizon framework. For example, if a decision-maker accepts high energy costs and emissions in the first decision horizon in favor of a low makespan, these are irreversible in subsequent decision horizons. When following an MS trajectory, the makespan of schedules remains stable across various decision horizons or may even decrease further, as the algorithm has additional computing time to explore the solution space with each successive horizon. When following an EC or EM trajectory, energy cost and emissions exhibit more dynamic behavior across the horizons. Due to uncertainties regarding the energy market and the generation of RES behind the meter, the algorithm updates forecasted energy prices and emissions over time and eventually replace them with the final actual values.

6.3. Practicality of schedules

In this section, we discuss the research question III and evaluate the practicality of the generated schedules. Given that the algorithm generates an estimated Pareto front comprising various schedules for each instance and case characteristic, we focus on selected examples of instance mk10. We select instance mk10 due to its characteristics as a medium-size instance with 20 distinct jobs, which provides a substantial energy demand. This allows us to observe how jobs and operations are assigned by Memetic NSGA-III based on the energy market conditions, consid-

ering the selected trajectory, and the interaction between ESS and RES facilitated by energy procurement decisions.

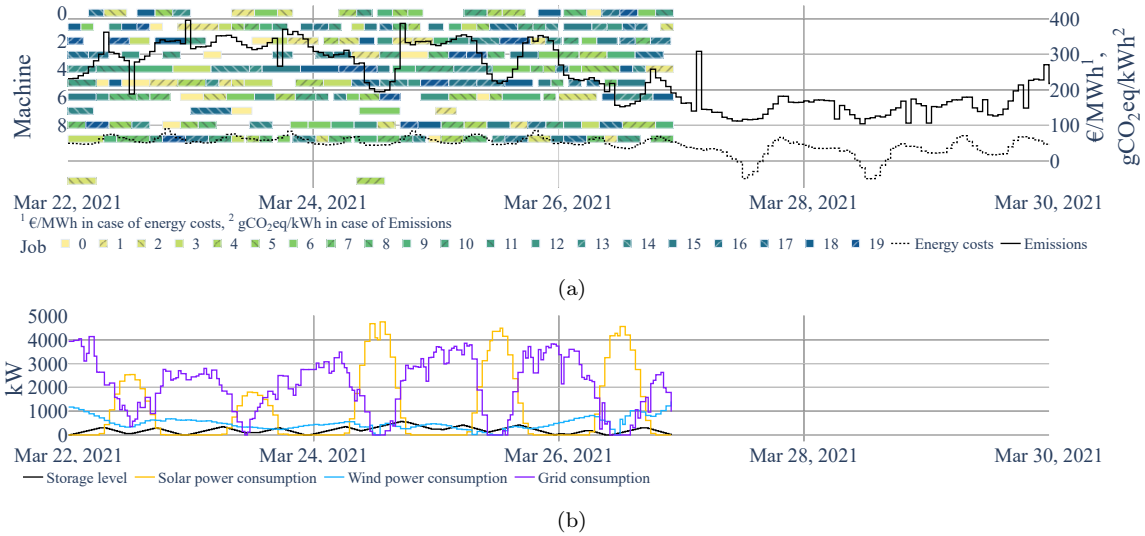

Figure 10: Gantt chart and energy procurement for mk10, makespan trajectory

Figures 10a to 12a show Gantt charts of instance mk10, corresponding to the MS, EC and TO trajectories, respectively. The x-axes represent the date, while the left y-axes display the machine assignments through horizontal bars, indicating the processing of operation. The right y-axes show the energy cost in €/MWh (dashed line) and the emissions in gCO_2eq/kWh (solid line). The depiction of market data aims to facilitate the understanding of periods that retroactively are favorable in terms of energy costs and emissions. Figures 10b and 11b show energy procurement decisions. Similarly to the Gantt charts, the x-axes show the date. The y-axes depict storage levels, self-generated solar and wind energy utilization, and grid-purchased energy in kW.

In Figure 10a, the schedule is generated with an MS trajectory and has a makespan of 237 time steps (4.9 days) with €14436.28 energy cost and 80.69 tCO_2eq emissions. The Gantt chart illustrates that the algorithm schedules all operations as early as possible to minimize the makespan, without considering energy costs or emissions. The corresponding energy procurement in Figure 10b shows a significant utilization of self-generated wind and solar energy to meet energy requirements. The level of the ESS indicates strategic charging during favorable times and discharging during periods of unfavorable market prices, thus minimizing the consumption of the grid to fulfill energy needs.

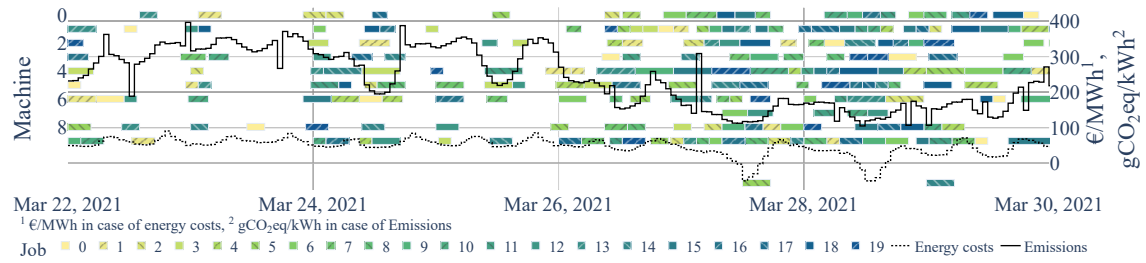

(a)

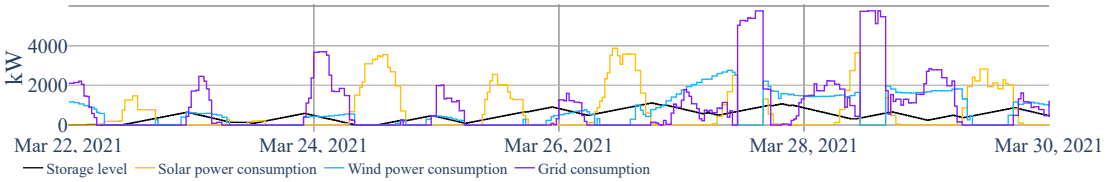

(b)

Figure 11: Gantt chart and energy procurement for mk10, energy cost trajectory

In Figure 11a, the schedule is generated with an EC trajectory and has a makespan of 416 time steps (8.67 days) with €3963.61 energy cost and 42.38 tCO_2eq emissions. Compared to the MS trajectory, this is an increase in makespan of 43.03% while reducing energy costs by 72.54% and emissions by 47.48%. The solution of EC trajectory allows for more idle times between operations, such as during the period from March 22 to March 26: The energy demand is met by RES generation when energy prices are high (e.g., during the daytime on March 23), and production halts when no own energy is produced (e.g., on the evening of March 23). In contrast, favorable times with low energy prices and high RES generation, such as those beginning March 22 at midnight and March 22 at noon, witness most machines in operation and energy drawn from the grid. Figure 11b illustrates that during these times, the algorithm maximizes the load on the grid, serves the most energy-intensive operations, and charges the energy storage system. Following these peak periods, production relies on the utilization of temporarily stored RES energy and self-generated ESS energy to meet its energy requirements.

Figure 12a shows a schedule based on the TO trajectory with a makespan of 317 (6.6 days) with €11138.75 energy cost and 69.58 tCO_2eq emissions. Compared to the MS trajectory, this is an increase in makespan of 25.24% while reducing energy costs by 22.84% and emissions by 13.77%. The schedule allows for faster completion compared to the EC trajectory, while introducing more idle times during periods of expensive energy prices and high emissions. This approach helps to reduce both

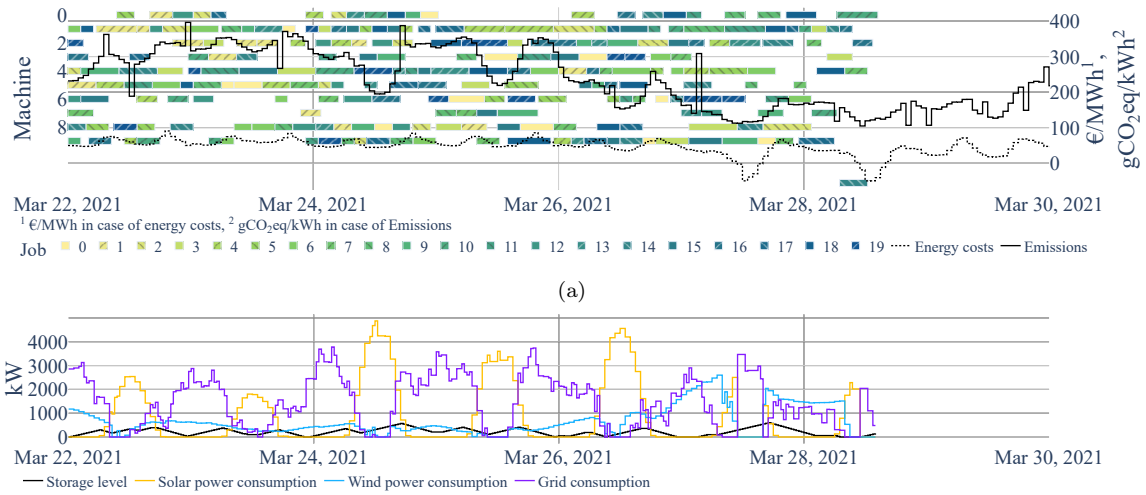

(a)

(b)

Figure 12: Gantt chart and energy procurement for mk10, trade-off trajectory

energy costs and emissions while decreasing the impact on the makespan. Figure 12b shows that energy procurement consistently chooses the most favorable energy mix, irrespective of the trajectory, thereby ensuring both low costs and low emissions in energy procurement.

With regard to the research question III – how feasible schedules based on energy cost and emissions are for practice – the two-level approach generates schedules that can be implemented in reality. We come to this conclusion, since the experiments reflect all possible extreme preferences of decision-makers (MS, EC, and EM trajectory) and show that feasible schedules can be designed for all cases. Accordingly, schedules can also be generated for all combinations of weightings, as the TO trajectory shows as an example for a decision-maker with balanced preferences. Given the variability across applications, a decision-maker benefits from the estimated Pareto front, which offers a range of possible schedules and allows for more nuanced considerations.

Beyond the mere feasibility of the calculated schedules, their acceptance in practical applications is also a crucial aspect to consider. The results indicate that as the makespan increases, additional idle time is introduced between the processing of operations, which, in turn, results in periods of worker inactivity. In practical applications, the acceptance of idle periods largely depends on the specific context of production planning. In some cases, these periods could be repurposed for activities such as maintenance or by reallocating workers to other tasks, ensuring that machine downtime aimed at reducing energy costs and emissions does not necessarily trans-

late into a complete production halt. However, if such redeployment strategies are not feasible or effective, decision-makers may prefer to avoid schedules with excessive interruptions, as this could lead to significantly reduced utilization rates. In such scenarios, while decision-makers can still leverage insights from the estimated Pareto front, they are likely to prioritize solutions with minimal makespan to maintain operational efficiency.

7. Conclusion

In this section, we summarize our contribution and its limitations and provide an outlook for future research avenues. Our research addresses the challenge faced by manufacturers in flexibly adapting their production schedules to fluctuations in energy prices and emissions while making energy procurement decisions. Our framework incorporates RTP tariffs to accommodate dynamic changes in energy prices and emissions, while also considering behind-the-meter RES and ESS assets. To aid decision-makers, we design a multi-objective NSGA-III algorithm to design production schedules, while we solve an EPP exactly using a state-of-the-art solver to guide energy procurement decisions. Through computational experiments, we explore (I) the sensitivity of our approach to seasonal variations, (II) the effects of different decision-makers' trajectories over time, and (III) the practicality of schedules based on minimizing energy costs or emissions. Based on our findings, we provide insights that empower manufacturers to estimate potential savings in flexible production based on energy price and emission values, and to devise more sustainable production schedules.

We see several possibilities for future research. A first line of research can expand the scope of research to incorporate additional requirements from manufacturers. For our computational experiments, we consider the requirements outlined by Brandimarte (1993) and extend the model to include constraints that reflect the dynamics of the energy market, RES generation, and ESS control. However, extending this work to real-world instances remains an important direction for future research. The literature contains additional constraints across various domains, such as time windows such as release and due dates (Tadumadze et al., 2020), sequence-dependent setup times and machine operator qualifications (Kress et al., 2019), or factors such as machine maintenance (Geurtsen et al., 2023). Therefore, we recommend creating more complex and diverse industrial scenarios through collaboration with industry. Subsequently, a case study can facilitate the application of the model to real-world decision-making scenarios, using empirical data to derive insights into energy-aware scheduling and procurement.

A second line of research can explore the interplay between our methodology and forecasted data. Although we use various forecasts for three distinct seasons, the impact of the quality of the forecasts on the results remains unknown. Further investigation could contrast the results assuming perfect knowledge with those derived from various accurate forecasts, measuring their effectiveness using metrics such as mean absolute percentage error (MAPE) or mean absolute deviation (MAD) (Wawale et al., 2022). In addition, Absi and van den Heuvel (2019) for example, conducted a worst-case analysis for decisions in the context of a lot-sizing problem and investigated how fixing decisions with a moving time window affects the solution quality. Further investigations could explore the impact of variable fixations after decision horizons and analyze how the accuracy of forecasts – whether overly pessimistic or optimistic – affects the outcomes.

Declarations

Funding

The authors appreciate the financial support provided by the state of North Rhine-Westphalia, Germany, as part of the *progres.nrw* program area, in the framework of Re^{2}Pli (project number EFO 0127A) and the funding of this project by computing time provided by the Paderborn Center for Parallel Computing (PC^2).

Competing interests

The authors declare that they have no known competing financial interests or personal relationships that could have appeared to influence the work reported in this paper.

Availability of data

The data that support the findings of this study are available from the corresponding author upon request.

Appendix A. Cases and forecasts

In this section, we complement the season introduction of Section 5.2, present the energy data for January and May 2021 in Appendix Appendix A.1 and give further information on forecast generation in Appendix Appendix A.2.

Appendix A.1. Cases

To accommodate fluctuations in renewable production and different energy price situations on the energy market, we employ data sourced from the Federal Network Agency Germany (2024) The datasets cover the period from October 1, 2018, to December 31, 2021, on an hourly basis and include day-ahead prices from the German wholesale market and actual net electricity generation data categorized by energy source. Figures A.13a and A.13b illustrate energy prices, while Figures A.14a and A.14b represent emissions for the January and May season. Figures A.15a and A.15b show the amount of energy generated by RES. The x-axes reflect the respective date and time, with the y-axes displaying costs in €/MWh, emissions in grams of carbon dioxide equivalent (gCO_2eq) per kWh, and kW generated by RES, respectively. The solid lines represent actual past values, while dashed lines depict the predicted values assumed at the beginning of each day for the decision horizons.

In January, energy costs fluctuate between €15.82 and €110.45, averaging at €110.45. Emissions vary from 129.38 gCO_2eq to 391.04 gCO_2eq, with an average of 285.35 gCO_2eq. RES production ranges from 0 kW to 1030.28 kW for solar and

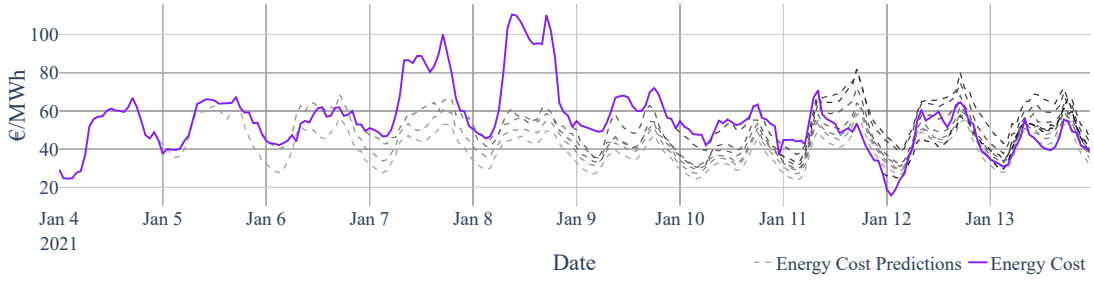

(a) January season

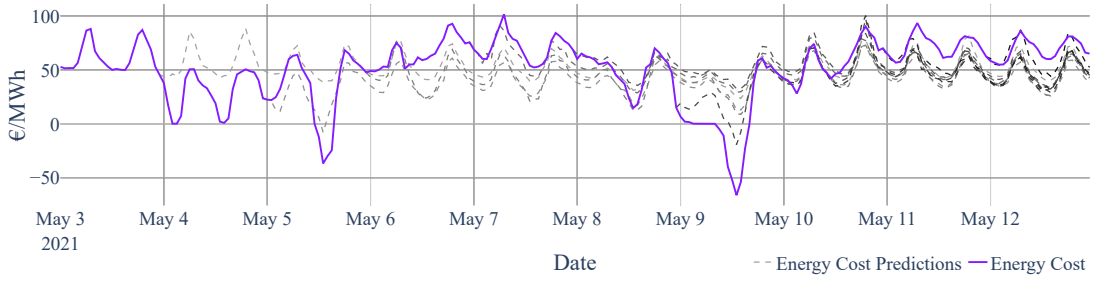

(b) May season

Figure A.13: Energy cost and predictions

127.86 kW to 2855.55 kW for wind, with mean values of 94.14 kW and 1009.05 kW, respectively. During the January season, RES generate a total of 264.77 MWh.

In March, energy costs span from -€49.99 to €96.80, averaging at €48.83. Emissions range between 104.54 gCO_2eq and 411.32 gCO_2eq, with an average of 245.41 gCO_2eq. RES production varies from 0 kW to 5430.48 kW for solar and 19.85 kW to 2758.63 kW for wind, with mean values of 1218.50 kW and 838.65 kW, respectively. During the March season, RES generate a total of 493.71 MWh.

In May, energy costs vary between -€66.18 and €101.50, averaging at €51.39. Emissions range from 85.04 gCO_2eq to 427.98 gCO_2eq, with an average of 204.73 gCO_2eq. RES production spans from 0 kW to 5589.08 kW for solar and 266.78 kW to 3367.66 kW for wind, with mean values of 1260.99 kW and 1293.55 kW, respectively. During the May season, RES generate a total of 613.09 MWh.

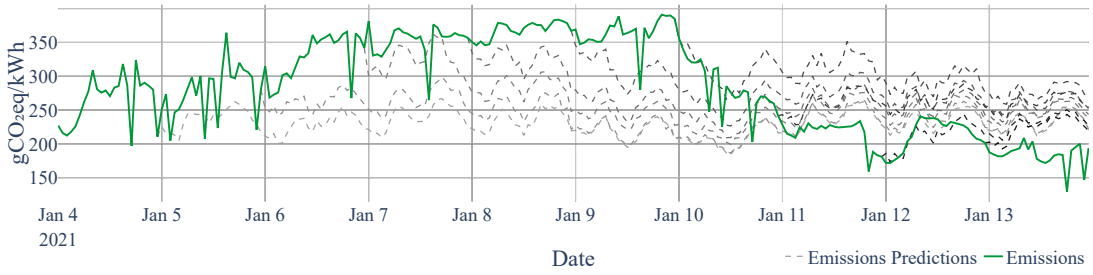

(a) January season

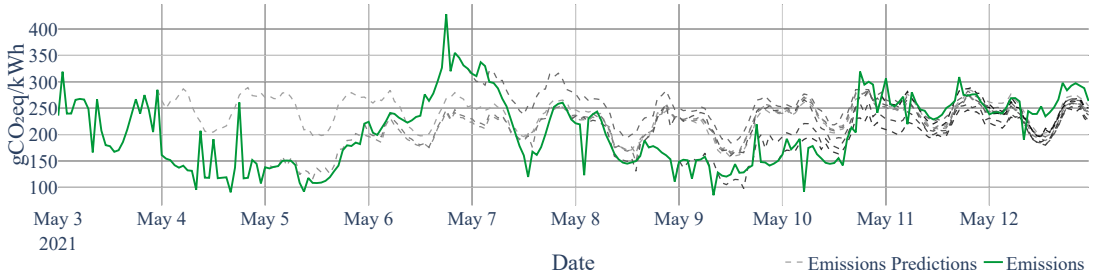

(b) May season

Figure A.14: Emissions and predictions

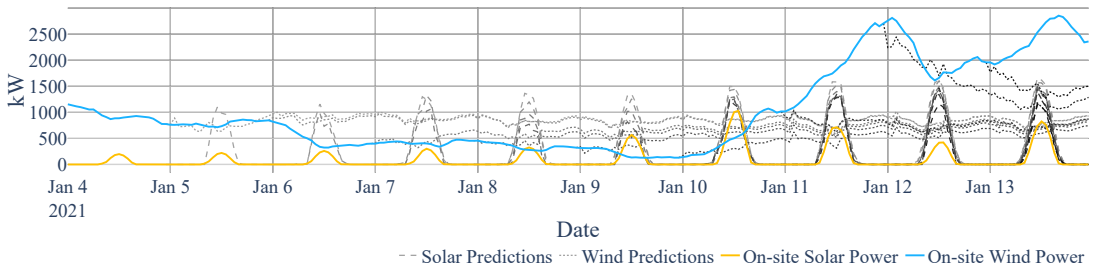

(a) January season

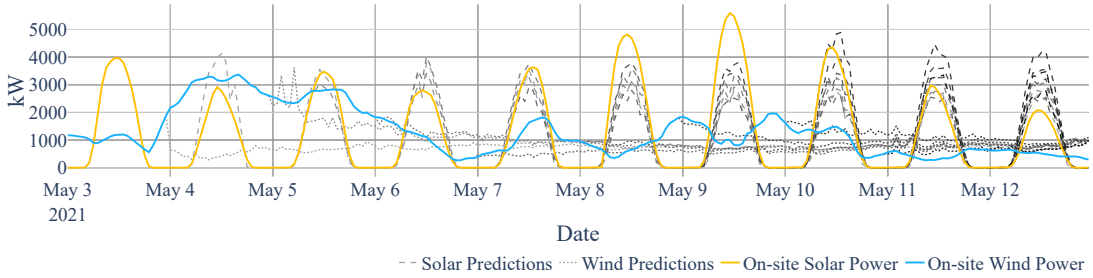

(b) May season

Figure A.15: Solar and wind generation and predictions

Appendix A.2. Forecast generation

The rolling-horizon approach requires uncertain energy prices, emissions, and RES generation for future time horizons, which are updated at the beginning of each horizon. We generate forecasts of future price, emissions, and RES generation trends for 10 consecutive days each from January, March, and May in 2021, utilizing the LEAR model of the *epftoolbox* (Lago et al., 2021). Since we do not use exogenous data, the LEAR model generates naive forecasts based on historical data patterns. As part of our analysis, we do not aim to use accurate forecasts but rather to draw patterns that we update on a daily basis and eventually assume known day-ahead prices. Thus, the rolling horizon approach can adjust to the disparities between the expected forecasts and the actual developments in energy cost, emissions, and RES generation. For practical implementation of our approach, we suggest incorporating relevant exogenous data to improve prediction accuracy when employing regression analysis techniques, such as the LEAR model. Alternatively, probabilistic price forecasting methods, as demonstrated by Andrade et al. (2017) or Bello et al. (2016), can also be considered.

Appendix B. Result table for seasonal differences

In this section, we present the results of our experiments in addition to the results presented in Section 6.1. With respect to Section 6.1, Table B.6 shows the minimum, average, and maximum values of the objective function for the makespan, energy cost, and emissions. The table breaks down the results according to the data for the season considered (January, March, or May).

Table B.6: Results for different seasonal conditions

Instance	January			March			May		
	Min	Avg	Max	Min	Avg	Max	Min	Avg	Max
Makespan (time steps)									
mk01	57.00	72.00	83.00	57.00	63.60	69.00	48.00	56.70	69.00
mk02	33.00	43.50	53.00	34.00	40.70	48.00	38.00	41.50	48.00
mk03	250.00	276.50	312.00	234.00	251.90	273.00	211.00	236.70	263.00
mk04	91.00	101.90	109.00	85.00	96.70	108.00	80.00	89.80	107.00
mk05	218.00	248.20	272.00	203.00	220.80	241.00	209.00	218.90	236.00
mk06	103.00	125.80	151.00	108.00	121.60	135.00	81.00	101.50	124.00
mk07	216.00	224.20	235.00	191.00	206.70	229.00	165.00	192.40	214.00
mk08	620.00	647.80	720.00	577.00	604.40	647.00	560.00	577.80	595.00
mk09	363.00	454.10	527.00	357.00	392.00	431.00	339.00	364.30	440.00
mk10	355.00	389.00	439.00	317.00	345.70	366.00	282.00	299.80	327.00
mk11	676.00	762.00	814.00	695.00	715.10	745.00	685.00	696.00	713.00
mk12	646.00	689.80	743.00	615.00	658.50	715.00	573.00	599.40	637.00
mk13	591.00	622.40	658.00	547.00	591.80	638.00	470.00	515.60	594.00
mk14	794.00	861.60	937.00	758.00	796.00	822.00	718.00	775.10	828.00
mk15	461.00	470.20	478.00	420.00	451.20	476.00	416.00	436.30	470.00
Energy cost (t€)									
mk01	1.26	1.47	1.85	1.07	1.45	1.65	0.08	0.21	0.34
mk02	1.40	1.60	1.78	1.34	1.50	1.68	0.27	0.52	0.66
mk03	6.85	7.52	9.05	4.42	5.12	5.77	0.61	0.93	1.39
mk04	3.99	4.55	5.14	3.07	3.87	4.53	0.28	0.62	0.88
mk05	4.46	4.79	5.17	2.94	3.39	3.59	0.32	0.61	0.93
mk06	4.26	5.18	6.62	2.88	3.92	4.76	-0.17	0.41	1.20
mk07	7.51	8.95	10.50	2.63	3.42	4.10	0.31	0.96	1.63
mk08	11.01	11.67	12.51	5.49	6.14	6.86	1.68	2.28	3.06
mk09	9.60	9.96	10.56	6.60	7.51	7.90	1.13	1.41	2.03
mk10	16.23	17.61	21.28	7.02	9.66	12.41	3.01	5.44	6.43
mk11	10.27	12.40	14.59	4.30	5.06	5.85	0.99	1.91	2.37
mk12	12.84	14.81	15.73	5.67	7.49	9.13	2.59	3.55	4.40
mk13	17.81	18.79	19.75	8.45	10.78	12.21	4.73	5.32	6.34
mk14	18.57	20.57	22.28	9.00	10.50	11.54	3.18	4.69	6.65
mk15	39.14	41.56	44.09	24.38	25.37	26.94	19.44	22.16	25.09
Emissions (tCO_2eq)									
mk01	8.41	9.36	11.42	7.94	9.79	11.03	2.72	3.19	3.65
mk02	9.21	10.01	10.76	8.63	9.47	10.29	3.29	4.29	4.76
mk03	43.09	46.16	54.13	29.54	32.56	35.96	11.85	13.07	15.30
mk04	26.50	28.50	30.26	20.48	24.33	27.42	7.29	8.43	9.88
mk05	27.79	29.02	29.95	19.58	21.80	22.94	7.06	8.29	9.18
mk06	27.88	32.51	39.44	19.35	25.35	29.98	7.01	9.47	12.55
mk07	46.90	55.60	62.82	27.25	30.20	32.47	16.04	18.21	20.30
mk08	64.61	68.40	70.76	35.89	40.05	43.44	16.39	18.97	21.43
mk09	56.60	58.95	61.61	41.58	45.64	47.64	14.99	16.04	18.71
mk10	99.48	106.64	121.43	51.79	63.30	74.97	31.44	35.90	39.14
mk11	63.82	72.58	81.33	35.77	38.12	41.48	19.36	21.68	22.89
mk12	81.09	86.57	90.03	41.62	49.37	56.72	23.26	26.99	30.23
mk13	106.35	109.49	113.15	55.39	65.64	72.58	32.30	34.85	38.99
mk14	113.55	124.13	133.09	69.04	72.74	75.19	38.73	43.02	49.12
mk15	222.31	235.49	244.71	147.94	154.78	164.17	113.01	119.50	125.96

Appendix C. Results for decision trajectories

In this section, we complement the results presented in Section 6.2 and show results on the average objective function values of all horizons for all instances. The line charts show the progression of objective function values over several horizons of the rolling horizon approach. Since we chose a horizon length of one day, horizon 0 reflects the anticipated objective function values at the end of the first day, while the final objective function values are shown at each curve's endpoint. The color of a line represents the decision-makers' trajectory: black lines depict an MS trajectory, purple lines depict an EC trajectory, green lines depict an EM trajectory, and yellow lines depict an TO trajectory.

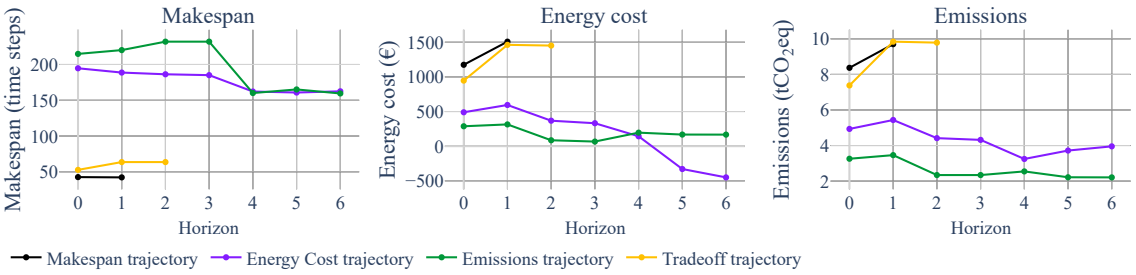

Figure C.16: Objective function values of mk01 for different trajectories over multiple horizons

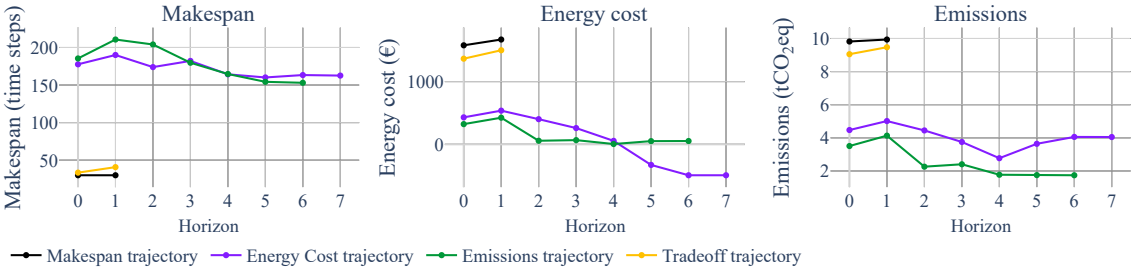

Figure C.17: Objective function values of mk02 for different trajectories over multiple horizons

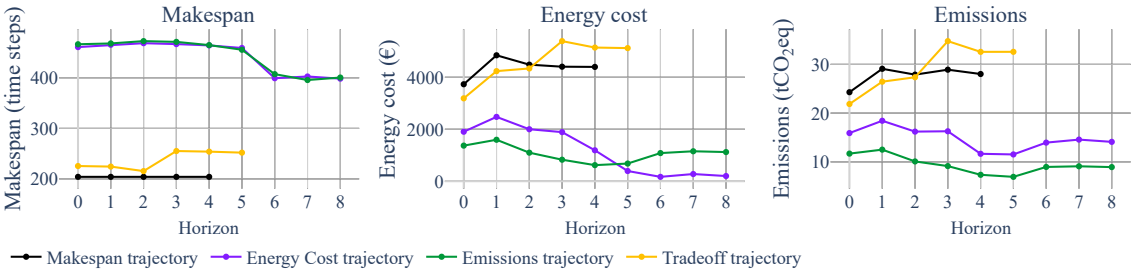

Figure C.18: Objective function values of mk03 for different trajectories over multiple horizons

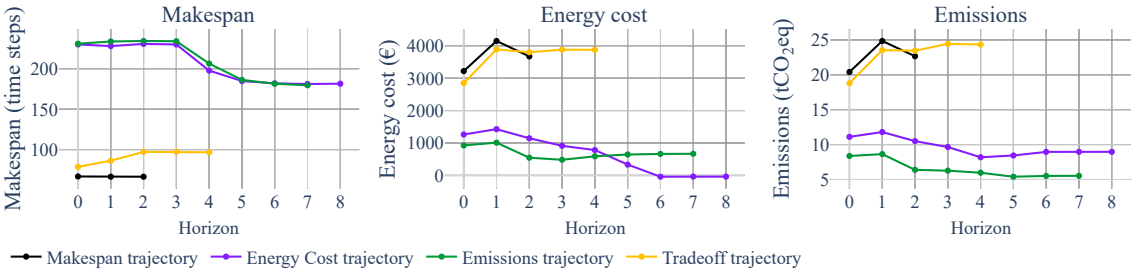

Figure C.19: Objective function values of mk04 for different trajectories over multiple horizons

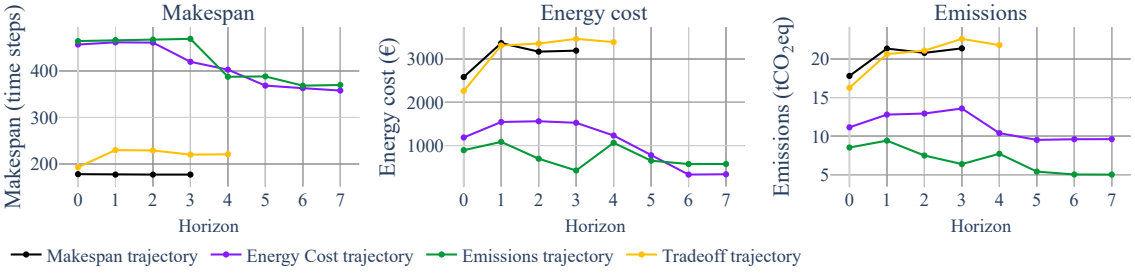

Figure C.20: Objective function values of mk05 for different trajectories over multiple horizons

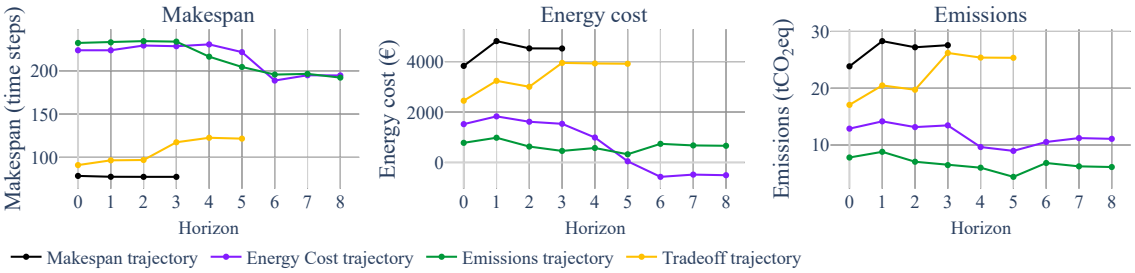

Figure C.21: Objective function values of mk06 for different trajectories over multiple horizons

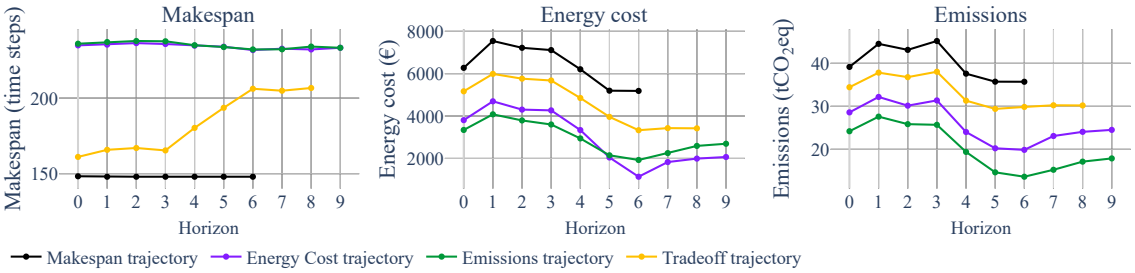

Figure C.22: Objective function values of mk07 for different trajectories over multiple horizons

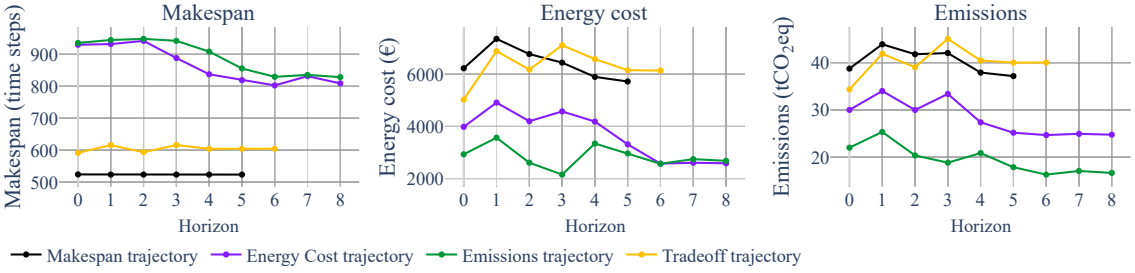

Figure C.23: Objective function values of mk08 for different trajectories over multiple horizons

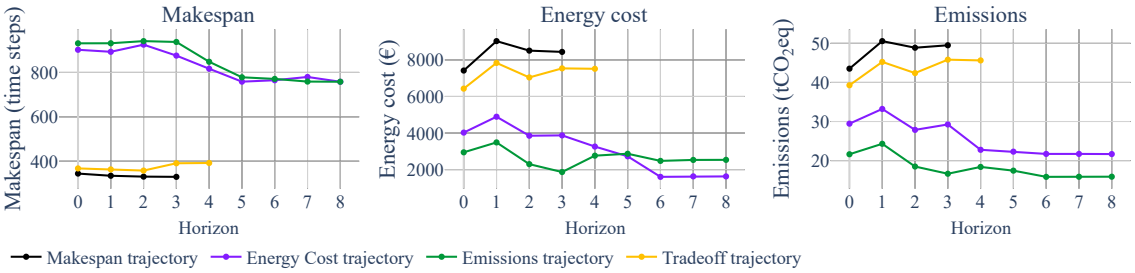

Figure C.24: Objective function values of mk09 for different trajectories over multiple horizons

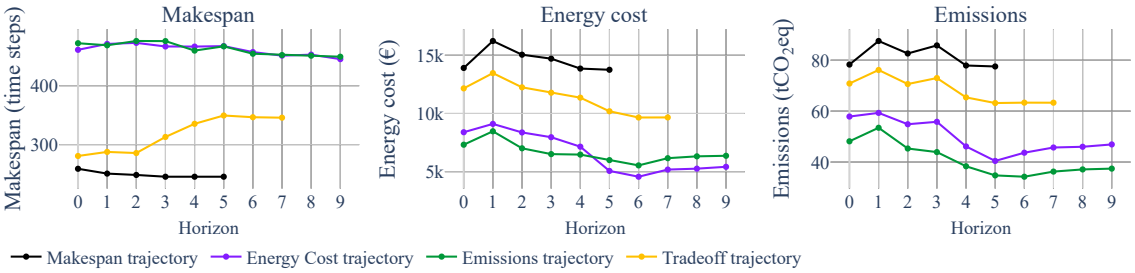

Figure C.25: Objective function values of mk10 for different trajectories over multiple horizons

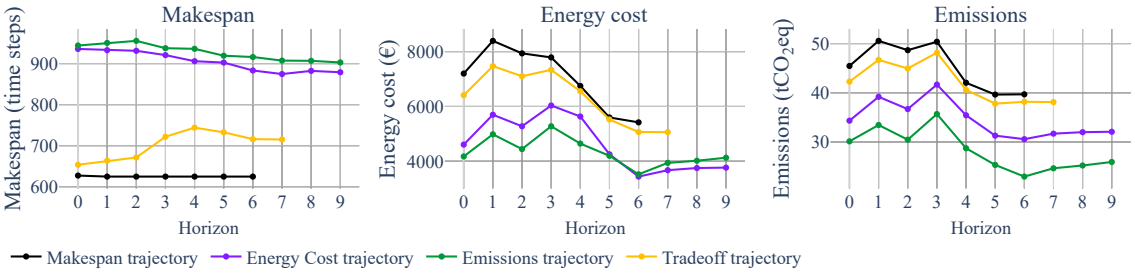

Figure C.26: Objective function values of mk11 for different trajectories over multiple horizons

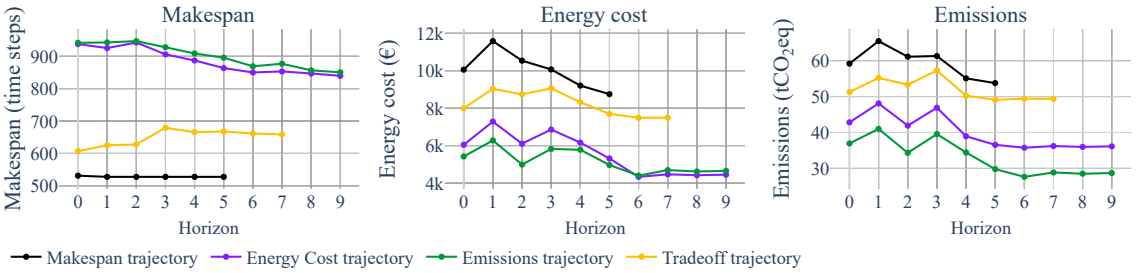

Figure C.27: Objective function values of mk12 for different trajectories over multiple horizons

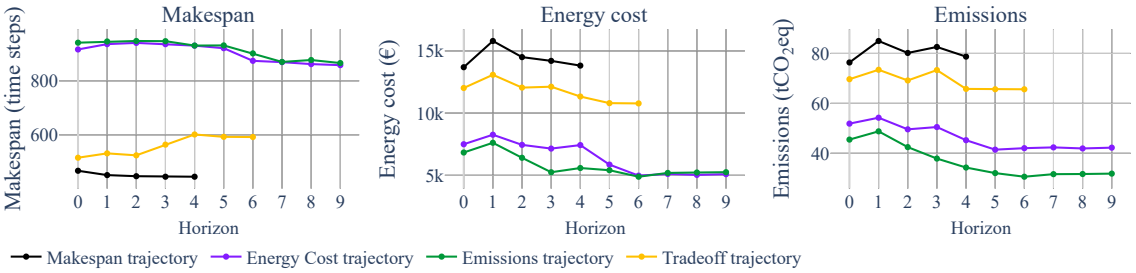

Figure C.28: Objective function values of mk13 for different trajectories over multiple horizons

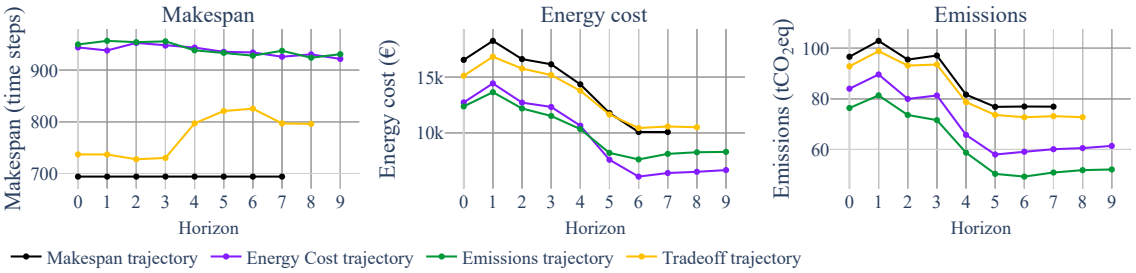

Figure C.29: Objective function values of mk14 for different trajectories over multiple horizons

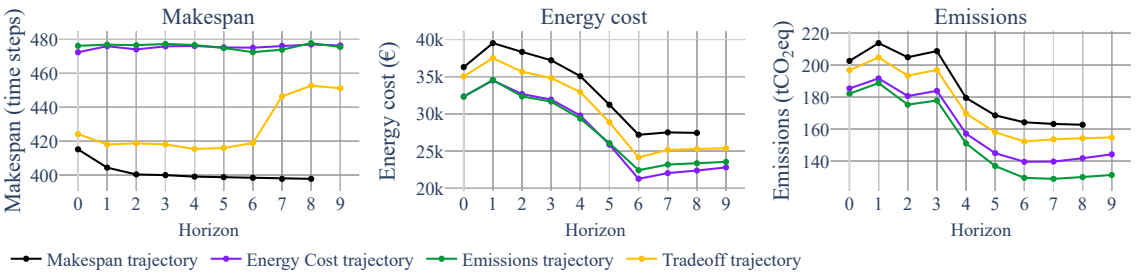

Figure C.30: Objective function values of mk15 for different trajectories over multiple horizons

Table C.7 breaks down the results according to the trajectory pursued during the solution process (trade-off, makespan, energy cost or emissions). With respect to Section 6.2, Table C.7 shows the minimum, average, and maximum values of the objective function for the makespan, energy cost, and emissions.

Table C.7: Results for different trajectories

Instance	Makespan			Energy Cost			Emissions			Trade-off		
	Min	Avg	Max	Min	Avg	Max	Min	Avg	Max	Min	Avg	Max
Makespan (time steps)												
mk01	41.00	42.20	43.00	156.00	162.50	167.00	143.00	159.50	173.00	57.00	63.60	69.00
mk02	28.00	29.90	31.00	153.00	162.60	175.00	144.00	153.00	160.00	34.00	40.70	48.00
mk03	204.00	204.00	204.00	365.00	398.30	416.00	372.00	400.50	421.00	234.00	251.90	273.00
mk04	65.00	66.50	69.00	171.00	181.50	203.00	170.00	179.50	191.00	85.00	96.70	108.00
mk05	174.00	177.20	182.00	337.00	357.80	374.00	355.00	369.80	384.00	203.00	220.80	241.00
mk06	73.00	77.40	82.00	185.00	194.70	210.00	178.00	192.20	213.00	108.00	121.60	135.00
mk07	144.00	148.00	156.00	222.00	233.30	239.00	229.00	233.30	239.00	191.00	206.70	229.00
mk08	523.00	523.50	526.00	742.00	808.80	857.00	789.00	828.30	868.00	577.00	604.40	647.00
mk09	319.00	329.50	343.00	707.00	758.00	787.00	740.00	758.10	799.00	357.00	392.00	431.00
mk10	237.00	245.50	254.00	416.00	445.10	461.00	422.00	449.20	469.00	317.00	345.70	366.00
mk11	616.00	624.70	633.00	824.00	879.00	922.00	846.00	902.90	941.00	695.00	715.10	745.00
mk12	524.00	527.60	540.00	784.00	839.70	886.00	806.00	850.40	919.00	615.00	658.50	715.00
mk13	436.00	444.80	450.00	815.00	858.10	908.00	816.00	865.90	910.00	547.00	591.80	638.00
mk14	694.00	694.00	694.00	908.00	921.70	941.00	914.00	930.90	951.00	758.00	796.00	822.00
mk15	390.00	397.80	410.00	470.00	476.40	479.00	470.00	475.50	479.00	420.00	451.20	476.00
Energy cost (t€)												
mk01	1.42	1.51	1.65	-0.61	-0.45	-0.32	0.03	0.17	0.56	1.07	1.45	1.65
mk02	1.58	1.67	1.80	-0.80	-0.49	-0.09	0.01	0.05	0.10	1.34	1.50	1.68
mk03	4.20	4.40	4.56	-0.48	0.20	0.65	0.40	1.12	2.03	4.42	5.12	5.77
mk04	3.49	3.67	3.98	-0.49	-0.04	0.65	0.30	0.67	1.21	3.07	3.87	4.53
mk05	3.03	3.19	3.44	-0.33	0.34	0.82	0.21	0.57	0.75	2.94	3.39	3.59
mk06	3.80	4.52	4.85	-0.84	-0.51	0.22	0.26	0.66	0.99	2.88	3.92	4.76
mk07	4.00	5.19	5.88	1.34	2.07	3.32	1.84	2.69	3.09	2.63	3.42	4.10
mk08	5.30	5.72	6.74	0.60	2.59	4.21	1.48	2.68	3.48	5.49	6.14	6.86
mk09	7.61	8.44	9.01	0.16	1.63	3.05	1.68	2.53	3.49	6.60	7.51	7.90
mk10	12.88	13.75	14.44	3.96	5.42	6.66	5.16	6.36	7.24	7.02	9.66	12.41
mk11	5.03	5.42	5.70	3.01	3.76	5.21	2.91	4.13	4.89	4.30	5.06	5.85
mk12	7.70	8.75	9.16	2.70	4.45	5.89	3.35	4.65	5.55	5.67	7.49	9.13
mk13	13.19	13.82	14.33	3.28	5.09	6.26	4.35	5.25	6.10	8.45	10.78	12.21
mk14	9.49	10.08	10.51	5.69	6.66	7.86	7.15	8.29	9.14	9.00	10.50	11.54
mk15	26.45	27.45	28.58	21.10	22.81	24.94	22.61	23.55	25.13	24.38	25.37	26.94
Emissions (tCO_2eq)												
mk01	9.28	9.70	10.44	3.50	3.95	4.35	1.47	2.21	4.21	7.94	9.79	11.03
mk02	9.54	9.94	10.55	3.23	4.05	4.79	1.46	1.74	1.95	8.63	9.47	10.29
mk03	26.97	28.01	28.96	11.55	14.11	16.87	5.66	8.93	12.54	29.54	32.56	35.96
mk04	21.57	22.66	24.19	7.49	8.96	11.02	3.99	5.52	7.92	20.48	24.33	27.42
mk05	20.44	21.38	22.68	7.56	9.61	12.51	3.55	5.02	5.63	19.58	21.80	22.94
mk06	24.51	27.58	29.16	9.18	11.08	13.44	3.80	6.12	7.77	19.35	25.35	29.98
mk07	29.99	35.71	39.33	20.93	24.52	30.41	12.97	17.88	20.15	27.25	30.20	32.47
mk08	35.42	37.16	41.19	17.84	24.75	31.48	11.88	16.66	19.69	35.89	40.05	43.44
mk09	45.71	49.51	51.92	19.20	21.67	25.20	12.52	15.88	20.09	41.58	45.64	47.64
mk10	72.46	77.52	80.93	42.37	46.92	52.86	32.99	37.42	41.29	51.79	63.30	74.97
mk11	38.58	39.69	40.76	28.53	32.08	37.70	20.68	25.94	29.82	35.77	38.12	41.48
mk12	50.75	53.74	55.78	30.35	36.14	42.60	22.78	28.72	34.29	41.62	49.37	56.72
mk13	75.70	78.72	81.39	36.13	42.26	46.65	28.38	31.86	35.57	55.39	65.64	72.58
mk14	74.67	76.91	79.29	57.63	61.40	63.16	48.81	52.10	55.39	69.04	72.74	75.19
mk15	158.49	162.74	167.00	135.84	144.25	154.04	125.06	131.34	141.20	147.94	154.78	164.17

References

Abikarram, J.B., McConky, K., Proano, R., 2019. Energy cost minimization for unrelated parallel machine scheduling under real time and demand charge pricing. Journal of cleaner production 208, 232–242. doi:10.1016/j.jclepro.2018.10.048.

Absi, N., van den Heuvel, W., 2019. Worst case analysis of relax and fix heuristics for lot-sizing problems. European Journal of Operational Research 279, 449–458. doi:10.1016/j.ejor.2019.06.010.

Andrade, J.R., Filipe, J., Reis, M., Bessa, R.J., 2017. Probabilistic price forecasting for day-ahead and intraday markets: Beyond the statistical model. Sustainability 9, 1990. doi:10.3390/su9111990.

Barco-Burgos, J., Bruno, J., Eicker, U., Saldaña-Robles, A., Alcántar-Camarena, V., 2022. Review on the integration of high-temperature heat pumps in district heating and cooling networks. Energy 239, 122378. doi:10.1016/j.energy.2021.122378.

Bello, A., Bunn, D., Reneses, J., Muñoz, A., 2016. Parametric density recalibration of a fundamental market model to forecast electricity prices. Energies 9, 959. doi:10.3390/en9110959.

Beraldi, P., Violi, A., Carrozzino, G., Bruni, M.E., 2017. The optimal electric energy procurement problem under reliability constraints. Energy Procedia 136, 283–289. doi:10.1016/j.egypro.2017.10.244.

Bertsimas, D., Brown, D.B., Caramanis, C., 2011. Theory and applications of robust optimization. SIAM review 53, 464–501. doi:10.1137/080734510.

Biel, K., Zhao, F., Sutherland, J.W., Glock, C.H., 2018. Flow shop scheduling with grid-integrated onsite wind power using stochastic MILP. International Journal of Production Research 56, 2076–2098. doi:10.1080/00207543.2017.1351638.

Brandimarte, P., 1993. Routing and scheduling in a flexible job shop by tabu search. Annals of Operations research 41, 157–183. doi:10.1007/BF02023073.

Burmeister, S.C., 2024. Green multi-objective flexible job shop scheduling - a memetic NSGA-III approach for flexible loads with real-time energy cost and emissions. arXiv preprint arXiv:2405.14339 [cs.NE] doi:10.48550/arXiv.2405.14339.

Burmeister, S.C., Guericke, D., Schryen, G., 2023. A memetic NSGA-II for the multi-objective flexible job shop scheduling problem with real-time energy tariffs. Flexible Services and Manufacturing Journal doi:10.1007/s10696-023-09517-7.

Che, A., Zhang, S., Wu, X., 2017. Energy-conscious unrelated parallel machine scheduling under time-of-use electricity tariffs. Journal of cleaner production 156, 688–697. doi:10.1016/j.jclepro.2017.04.018.

Chen, W., Wang, J., Yu, G., 2022. Energy-efficient scheduling for an energy-intensive industry under punitive electricity price. Journal of Cleaner Production 373, 133851. doi:10.1016/j.jclepro.2022.133851.

Conejo, A., Fernandez-Gonzalez, J., Alguacil, N., 2005. Energy procurement for large consumers in electricity markets. IEE Proceedings-Generation, Transmission and Distribution 152, 357–364. doi:10.1049/ip-gtd:20041252.

Cui, W., Li, L., Lu, Z., 2019. Energy-efficient scheduling for sustainable manufacturing systems with renewable energy resources. Naval Research Logistics (NRL) 66, 154–173. doi:10.1002/nav.21830.

Dai, M., Tang, D., Giret, A., Salido, M.A., 2019. Multi-objective optimization for energy-efficient flexible job shop scheduling problem with transportation constraints. Robotics and Computer-Integrated Manufacturing 59, 143–157. doi:10.1016/j.rcim.2019.04.006.

Deb, K., Jain, H., 2013. An evolutionary many-objective optimization algorithm using reference-point-based nondominated sorting approach, part I: solving problems with box constraints. IEEE transactions on evolutionary computation 18, 577–601. doi:10.1109/TEVC.2013.2281535.

Ding, J.Y., Song, S., Zhang, R., Chiong, R., Wu, C., 2015. Parallel machine scheduling under time-of-use electricity prices: New models and optimization approaches. IEEE Transactions on Automation Science and Engineering 13, 1138–1154. doi:10.1109/TASE.2015.2495328.

Dong, J., Ye, C., 2022. Green scheduling of distributed two-stage reentrant hybrid flow shop considering distributed energy resources and energy storage system. Computers & Industrial Engineering 169, 108146. doi:10.1016/j.cie.2022.108146.

Duarte, J.L.R., Fan, N., Jin, T., 2020. Multi-process production scheduling with variable renewable integration and demand response. European Journal of Operational Research 281, 186–200. doi:10.1016/j.ejor.2019.08.017.

Elbersen, B., Staritsky, I., Hengeveld, G., Schelhaas, M., Naeff, H., Böttcher, H., 2012. Atlas of EU biomass potentials: spatially detailed and quantified overview

of EU biomass potential taking into account the main criteria determining biomass availability from different sources. IEE 08653 S12.529 241, IIASA.

Fang, K., Uhan, N., Zhao, F., Sutherland, J.W., 2011. A new approach to scheduling in manufacturing for power consumption and carbon footprint reduction. Journal of Manufacturing Systems 30, 234–240. doi:10.1016/j.jmsy.2011.08.004.

Fazli Khalaf, A., Wang, Y., 2018. Energy-cost-aware flow shop scheduling considering intermittent renewables, energy storage, and real-time electricity pricing. International Journal of Energy Research 42, 3928–3942. doi:10.1002/er.4130.

Federal Network Agency Germany, 2024. SMARD market data. online. URL: https://www.smard.de/en/downloadcenter/download-market-data.

Garey, M.R., Johnson, D.S., Sethi, R., 1976. The complexity of flowshop and jobshop scheduling. Mathematics of operations research 1, 117–129. doi:10.1287/moor.1.2.117.

Geurtsen, M., Adan, J., Akçay, A., 2023. Integrated maintenance and production scheduling for unrelated parallel machines with setup times. Flexible Services and Manufacturing Journal , 1–34doi:10.1007/s10696-023-09511-z.

Glomb, L., Liers, F., Rösel, F., 2022. A rolling-horizon approach for multi-period optimization. European Journal of Operational Research 300, 189–206. doi:10.1016/j.ejor.2021.07.043.

Golpîra, H., Khan, S.A.R., Zhang, Y., 2018. Robust smart energy efficient production planning for a general job-shop manufacturing system under combined demand and supply uncertainty in the presence of grid-connected microgrid. Journal of cleaner production 202, 649–665. doi:10.1016/j.jclepro.2018.08.151.

Gong, G., Deng, Q., Gong, X., Huang, D., 2021. A non-dominated ensemble fitness ranking algorithm for multi-objective flexible job-shop scheduling problem considering worker flexibility and green factors. Knowledge-Based Systems 231, 107430. doi:10.1016/j.knosys.2021.107430.

Gong, G., Deng, Q., Gong, X., Liu, W., Ren, Q., 2018. A new double flexible job-shop scheduling problem integrating processing time, green production, and human factor indicators. Journal of Cleaner Production 174, 560–576. doi:10.1016/j.jclepro.2017.10.188.

Gong, X., De Pessemier, T., Joseph, W., Martens, L., 2015. An energy-cost-aware scheduling methodology for sustainable manufacturing. Procedia CIRP 29, 185–190. doi:10.1016/j.procir.2015.01.041.

Gong, X., De Pessemier, T., Joseph, W., Martens, L., 2016. A generic method for energy-efficient and energy-cost-effective production at the unit process level. Journal of Cleaner Production 113, 508–522. doi:10.1016/j.jclepro.2015.09.020.

Hassan, Q., Nassar, A.K., Al-Jiboory, A.K., Viktor, P., Telba, A.A., Awwad, E.M., Amjad, A., Fakhruldeen, H.F., Algburi, S., Mashkoor, S.C., et al., 2024. Mapping europe renewable energy landscape: Insights into solar, wind, hydro, and green hydrogen production. Technology in Society 77, 102535. doi:10.1016/j.techsoc.2024.102535.

Huang, W., Zhang, N., Kang, C., Li, M., Huo, M., 2019. From demand response to integrated demand response: Review and prospect of research and application. Protection and Control of Modern Power Systems 4, 1–13. doi:10.1186/s41601-019-0126-4.

Ishibuchi, H., Tsukamoto, N., Nojima, Y., 2008. Evolutionary many-objective optimization: A short review, in: 2008 IEEE congress on evolutionary computation (IEEE world congress on computational intelligence), IEEE. pp. 2419–2426. doi:10.1109/CEC.2008.4631121.

Jabeur, M.H., Mahjoub, S., Toublanc, C., Cariou, V., 2024. Optimizing integrated lot sizing and production scheduling in flexible flow line systems with energy scheme: A two level approach based on reinforcement learning. Computers & Industrial Engineering , 110095doi:10.1016/j.cie.2024.110095.

Jiang, T., Zhang, C., Sun, Q.M., 2019. Green job shop scheduling problem with discrete whale optimization algorithm. IEEE Access 7, 43153–43166. doi:10.1109/ACCESS.2019.2908200.

Jordehi, A.R., 2019. Optimisation of demand response in electric power systems, a review. Renewable and sustainable energy reviews 103, 308–319. doi:10.1016/j.rser.2018.12.054.

Karimi, S., Kwon, S., 2021. Comparative analysis of the impact of energy-aware scheduling, renewable energy generation, and battery energy storage on production scheduling. International Journal of Energy Research 45, 18981–18998. doi:10.1002/er.6999.

Körner, M.F., Bauer, D., Keller, R., Rösch, M., Schlereth, A., Simon, P., Bauernhansl, T., Fridgen, G., Reinhart, G., 2019. Extending the automation pyramid for industrial demand response. Procedia CIRP 81, 998–1003. doi:10.1016/j.procir.2019.03.241.

Kress, D., Müller, D., Nossack, J., 2019. A worker constrained flexible job shop scheduling problem with sequence-dependent setup times. OR spectrum 41, 179–217. doi:10.1007/s00291-018-0537-z.

Lago, J., Marcjasz, G., De Schutter, B., Weron, R., 2021. Forecasting day-ahead electricity prices: A review of state-of-the-art algorithms, best practices and an open-access benchmark. Applied Energy 293, 116983. doi:10.1016/j.apenergy.2021.116983.

Lee, S., Do Chung, B., Jeon, H.W., Chang, J., 2017. A dynamic control approach for energy-efficient production scheduling on a single machine under time-varying electricity pricing. Journal of Cleaner Production 165, 552–563. doi:10.1016/j.jclepro.2017.07.102.

Leo, E., Dalle Ave, G., Harjunkoski, I., Engell, S., 2021. Stochastic short-term integrated electricity procurement and production scheduling for a large consumer. Computers & Chemical Engineering 145, 107191. doi:10.1016/j.compchemeng.2020.107191.

Li, H., Deb, K., Zhang, Q., Suganthan, P.N., Chen, L., 2019. Comparison between moea/d and nsga-iii on a set of novel many and multi-objective benchmark problems with challenging difficulties. Swarm and Evolutionary Computation 46, 104–117. doi:0.1016/j.swevo.2019.02.003.

Li, Y., Huang, W., Wu, R., Guo, K., 2020. An improved artificial bee colony algorithm for solving multi-objective low-carbon flexible job shop scheduling problem. Applied Soft Computing 95, 106544. doi:10.1016/j.asoc.2020.106544.

Lu, C., Zhang, B., Gao, L., Yi, J., Mou, J., 2021. A knowledge-based multiobjective memetic algorithm for green job shop scheduling with variable machining speeds. IEEE Systems Journal 16, 844–855. doi:10.1109/JSYST.2021.3076481.

Maia, R.G.T., Junior, A.O.P., Pessanha, J.F.M., Garcia, K.C., 2022. Methodology for setting corporate sustainability targets. Journal of Cleaner Production 369, 133359. doi:10.1016/j.jclepro.2022.133359.

Mancò, G., Tesio, U., Guelpa, E., Verda, V., 2024. A review on multi energy systems modelling and optimization. Applied Thermal Engineering 236, 121871. doi:10.1016/j.applthermaleng.2023.121871.

Marquant, J.F., Evins, R., Carmeliet, J., 2015. Reducing computation time with a rolling horizon approach applied to a milp formulation of multiple urban energy hub system. Procedia Computer Science 51, 2137–2146. doi:10.1016/j.procs.2015.05.486.

Masmoudi, O., Delorme, X., Gianessi, P., 2019. Job-shop scheduling problem with energy consideration. International Journal of Production Economics 216, 12–22. doi:10.1016/j.ijpe.2019.03.021.

Mitra, S., Sun, L., Grossmann, I.E., 2013. Optimal scheduling of industrial combined heat and power plants under time-sensitive electricity prices. Energy 54, 194–211. doi:10.1016/j.energy.2013.02.030.

Moon, J.Y., Park, J., 2014. Smart production scheduling with time-dependent and machine-dependent electricity cost by considering distributed energy resources and energy storage. International Journal of Production Research 52, 3922–3939. doi:10.1080/00207543.2013.860251.

Myszkowski, P.B., Laszczyk, M., 2021. Diversity based selection for many-objective evolutionary optimisation problems with constraints. Information Sciences 546, 665–700. doi:10.1016/j.ins.2020.08.118.

Obi, M., Slay, T., Bass, R., 2020. Distributed energy resource aggregation using customer-owned equipment: A review of literature and standards. Energy Reports 6, 2358–2369. doi:10.1016/j.egyr.2020.08.035.

Özgüven, C., Özbakır, L., Yavuz, Y., 2010. Mathematical models for job-shop scheduling problems with routing and process plan flexibility. Applied Mathematical Modelling 34, 1539–1548. doi:10.1016/j.apm.2009.09.002.

Panda, S., Mohanty, S., Rout, P.K., Sahu, B.K., Parida, S.M., Samanta, I.S., Bajaj, M., Piecha, M., Blazek, V., Prokop, L., 2023. A comprehensive review on demand side management and market design for renewable energy support and integration. Energy Reports 10, 2228–2250. doi:10.1016/j.egyr.2023.09.049.

Schulz, S., Neufeld, J.S., Buscher, U., 2019. A multi-objective iterated local search algorithm for comprehensive energy-aware hybrid flow shop scheduling. Journal of cleaner production 224, 421–434. doi:10.1016/j.jclepro.2019.03.155.

Shrouf, F., Ordieres-Meré, J., García-Sánchez, A., Ortega-Mier, M., 2014. Optimizing the production scheduling of a single machine to minimize total energy consumption costs. Journal of Cleaner Production 67, 197–207. doi:10.1016/j.jclepro.2013.12.024.

Tadumadze, G., Emde, S., Diefenbach, H., 2020. Exact and heuristic algorithms for scheduling jobs with time windows on unrelated parallel machines. OR Spectrum 42, 461–497. doi:10.1007/s00291-020-00586-w.

Wang, L., Lu, Z., Ren, Y., 2019. A rolling horizon approach for production planning and condition-based maintenance under uncertain demand. Proceedings of the Institution of Mechanical Engineers, Part O: Journal of Risk and Reliability 233, 1014–1028. doi:10.1177/1748006X19853671.

Wang, L., et al., 2020a. Multi-objective optimization based on decomposition for flexible job shop scheduling under time-of-use electricity prices. Knowledge-Based Systems 204, 106177. doi:10.1016/j.knosys.2020.106177.

Wang, S., Mason, S.J., Gangammanavar, H., 2020b. Stochastic optimization for flow-shop scheduling with on-site renewable energy generation using a case in the united states. Computers & Industrial Engineering 149, 106812. doi:10.1016/j.cie.2020.106812.

Warren, P., 2014. A review of demand-side management policy in the uk. Renewable and Sustainable Energy Reviews 29, 941–951. doi:10.1016/j.rser.2013.09.009.

Wawale, S.G., Bisht, A., Vyas, S., Narawish, C., Ray, S., 2022. An overview: Modeling and forecasting of time series data using different techniques in reference to human stress. Neuroscience Informatics 2, 100052. doi:10.1016/j.neuri.2022.100052.

Wu, X., Shen, X., Cui, Q., 2018. Multi-objective flexible flow shop scheduling problem considering variable processing time due to renewable energy. Sustainability 10, 841. doi:10.3390/su10030841.

Wu, X., Sun, Y., 2018. A green scheduling algorithm for flexible job shop with energy-saving measures. Journal of cleaner production 172, 3249–3264. doi:10.1016/j.jclepro.2017.10.342.

Yasmin, R., Amin, B.R., Shah, R., Barton, A., 2024. A survey of commercial and industrial demand response flexibility with energy storage systems and renewable energy. Sustainability 16, 731. doi:10.3390/su16020731.

Yin, L., Li, X., Gao, L., Lu, C., Zhang, Z., 2017. A novel mathematical model and multi-objective method for the low-carbon flexible job shop scheduling problem. Sustainable Computing: Informatics and Systems 13, 15–30. doi:10.1016/j.suscom.2016.11.002.

Yuan, Y., Xu, H., Wang, B., Yao, X., 2015. A new dominance relation-based evolutionary algorithm for many-objective optimization. IEEE Transactions on Evolutionary Computation 20, 16–37. doi:10.1109/TEVC.2015.2420112.

Zhai, Y., Biel, K., Zhao, F., Sutherland, J.W., 2017. Dynamic scheduling of a flow shop with on-site wind generation for energy cost reduction under real time electricity pricing. CIRP Annals 66, 41–44. doi:10.1016/j.cirp.2017.04.099.

Zhang, H., Cai, J., Fang, K., Zhao, F., Sutherland, J.W., 2017. Operational optimization of a grid-connected factory with onsite photovoltaic and battery storage systems. Applied Energy 205, 1538–1547. doi:10.1016/j.apenergy.2017.08.140.

Zhang, H., Zhao, F., Fang, K., Sutherland, J.W., 2014. Energy-conscious flow shop scheduling under time-of-use electricity tariffs. CIRP Annals 63, 37–40. doi:10.1016/j.cirp.2014.03.011.

Zhang, H., Zhao, F., Sutherland, J.W., 2015. Energy-efficient scheduling of multiple manufacturing factories under real-time electricity pricing. CIRP Annals 64, 41–44. doi:10.1016/j.cirp.2015.04.049.

Zhang, J., Ding, G., Zou, Y., Qin, S., Fu, J., 2019. Review of job shop scheduling research and its new perspectives under industry 4.0. Journal of Intelligent Manufacturing 30, 1809–1830.

Zhang, Q., Cremer, J.L., Grossmann, I.E., Sundaramoorthy, A., Pinto, J.M., 2016. Risk-based integrated production scheduling and electricity procurement for continuous power-intensive processes. Computers & chemical engineering 86, 90–105. doi:10.1016/j.compchemeng.2015.12.015.